CEDD INNOVATION SERIES







Construction, Testing and Application of High Strength Steel in Pile Foundation

Foreword

Civil Engineering and Development Department (CEDD) is committed to advancing engineering excellence through innovation, collaboration and the adoption of Advanced Construction Materials (ACM) and technologies. As development in the Northern Metropolis (NM) gathers pace, the complex geological conditions comprising meta-sedimentary (MS) rocks in the region present both challenges and opportunities for more efficient and sustainable foundation engineering.

To support NM's developments, CEDD initiated a comprehensive trial piling programme to investigate pile performance in MS rocks, evaluate the use of ground-granulated blast-furnace slag (GGBS) concrete and grout, and demonstrate the application of high-strength steel as an ACM in pile foundations. By combining full-scale field trials with scientific investigation and the hands-on construction experience, the programme provides an evidence-based basis for advancing the use of high-strength steel in pile foundations amongst other achievements.

The successful construction and testing of pre-bored socketed S690 steel H-piles with GGBS grout at Fung Kong provide valuable experience in the practical application of high-strength steel, particularly in site welding, quality assurance and pile construction. Multiple pile testing methods and strain measurements using distributed fibre optic sensing technology enable a more detailed understanding of pile behaviour and load transfer. Together with the design examples presented in this publication, these findings illustrate how high-strength steel can be used effectively in pile foundations, with the potential to reduce material consumption, construction time, costs and associated carbon emissions.

I would like to commend the project teams for their dedication and tremendous efforts in addressing the technical and practical challenges of adopting high-strength steel in foundation works. I also extend my sincere appreciation to our partners in academia and the construction industry for their expertise and collaboration. The programme exemplifies the value of University–Government–Industry (UGI) partnerships in translating research into practical engineering applications.

This CEDD Innovation Series publication brings together the experience and lessons learnt from the construction, testing and application of high-strength steel in pile foundations at Fung Kong. It is intended to serve as a useful reference for engineers, contractors and other industry practitioners. I hope that sharing this experience will encourage wider adoption of high-strength steel as an ACM in pile foundations, contributing to more productive, cost-effective and sustainable infrastructure development in Hong Kong.



Mr. FONG Hok-shing, Michael, JP.
Director of the Civil Engineering and Development Department

CEDD

Executive summary

High-strength steel offers opportunities to improve the efficiency of pre-bored socketed H-pile foundations through increased structural capacity that results in pile number reduction. To demonstrate its practical application in support of the development in Hong Kong including the Northern Metropolis, the Geotechnical Engineering Office (GEO) of the Civil Engineering and Development Department (CEDD) led the construction and testing of three full-scale S690 pre-bored socketed steel H-piles at Fung Kong, with support from The Hong Kong Polytechnic University (PolyU) and Ove Arup & Partners Hong Kong Limited (Arup). These trials formed part of CEDD's wider trial piling programme investigating pile performance in meta-sedimentary (MS) rocks and the use of innovative materials and construction technologies.

The trials established practical experience in site welding, inspection and installation of S690 steel piles, together with the placement of low-carbon grout incorporating ground-granulated blast-furnace slag (GGBS) as a 75% replacement for cement. Site welds met the inspection requirements, and the adopted grout achieved satisfactory workability, bleeding and compressive strength performance. Single Osterberg-cell (O-cell), conventional kentledge and multi-level Y-Jack tests, supported by distributed fibre optic measurements, enabled detailed assessment of pile response and load transfer. The kentledge-tested pile sustained a maximum load of 19,000 kN, with maximum and residual settlements meeting the specified acceptance criteria. Rock–grout bond stresses above the presumed allowable values specified by the earlier MS rock design provisions were mobilised without signs of pile failure.

As part of the Study, complementary design assessments have been carried out to examine the benefits of using S690 and S960 steel in four foundation design scenarios. The Study has indicated saving of approximately 30% to 50% fewer piles can be obtained comparing with conventional S450 options. The examples illustrated opportunities for smaller pile caps and reduced construction effort, with potential savings in construction time, costs and embodied carbon. The Study has also explored the potential of high-strength steel to extend the application of socketed H-piles to heavily loaded foundations where large-diameter bored piles might otherwise be considered.

The S690 field trials and S690/S960 design examples provide a sound basis for considering the use of high-strength steel in future pile foundations. This publication documents the construction controls, testing approaches and design considerations needed to utilise the higher steel capacity effectively. Together with the enhanced rock-socket resistance stipulated in GEO TGN No. 53 (Issue 2), the potential and benefits of using high-strength steel could be fully unlocked.

Table of Contents

Foreword 1
Executive summary 2
1. Introduction 5
1.1 Potential applications in pile foundations 5
1.2 Pain points and study objectives 6
2. Trial Piling Works in the Northern Metropolis 7
2.1 Overview of the pile loading test programme in the Northern Metropolis 7
2.2 Trial piles using high-strength steel in Fung Kong 8
2.3 Site geology and ground investigation at Fung Kong 10
2.4 Design, construction and test arrangements of three trial piles 13
2.4.1 Design and construction of the trial piles 14
2.4.2 Instrumentation 16
3. Innovative applications in Fung Kong test piles 18
3.1 High-strength steel in construction 18
3.1.1 Site welding of high-strength steel piles 19
3.1.2 Importance of welding procedures from metallurgical perspective 20
3.1.3 Comparing welding procedures of S690 steel and normal grade steel 22
3.1.4 Robotic welding and process control 23
3.1.5 Training of welders and robotic welding operators 23
3.2 GGBS grout in pre-bored socketed H-piles 24
3.2.1 Lessons learned from GGBS concrete bored piles 25
3.2.2 GGBS grout mix at Fung Kong test site 25
3.3 Multiple pile testing methods 28
3.3.1 Test arrangement and loading procedures 28
3.3.2 Value of multiple testing methods 31
3.4 Fibre optic sensing technology 32
3.4.1 Benefits of fibre optic sensing in S690 trial piles 33
3.4.2 Details of fibre optic instrumentation at Fung Kong site 34
3.4.3 Example results 35
4. Unlocking potentials and benefits of high-strength steel H-piles – Design examples 37
4.1 Basis for a like-for-like comparison 37
4.2 Application scenarios and practical benefits for steel grades S690 and S960 40
4.2.1 Scenario 1: Pile foundation using S450, S690 and S960 piles for a building 40
4.2.2 Scenario 2: Socketed H-piles under vertical load with negative skin friction 42

4.2.3 Scenario 3: Hybrid upper-zone H-piles under combined axial load and bending...44
4.2.4 Scenario 4: High-strength steel H-piles as alternatives to large-diameter bored piles 46
4.3 Potential benefits of high-strength steel piles 47
5. Summary and way forward....47
References....49

1. Introduction

To pave the way for upcoming developments especially in the Northern Metropolis, the Geotechnical Engineering Office (GEO) of the Civil Engineering and Development Department (CEDD) initiated and led a comprehensive trial piling programme that included the construction, testing and application of high-strength steel piles. The high-strength steel pile trials were supported by The Hong Kong Polytechnic University (PolyU) and Ove Arup & Partners Hong Kong Limited (Arup), with the aim of gaining practical experience in the use of high-strength steel and demonstrating its potential to enhance efficiency and cost-effectiveness and reduce the environmental impacts of foundation works. The wider programme also investigated the geological conditions in the new development areas and their implications for the geotechnical capacity of pile foundations, providing supporting knowledge for the application of high-strength steel underground.

The benefits of adopting high-strength steel in aboveground structure have already been demonstrated in other construction applications, notably the Tseung Kwan O Cross Bay Link and Lung Yeuk Tau Interchange footbridge (Figure 1.1). These projects adopted high-strength steel and Ultra-high strength steel materials with yield strengths of 690 MPa to 960 MPa, resulting in reduced material consumption, improved site logistics and lower construction costs. They have also become iconic structures in the region.



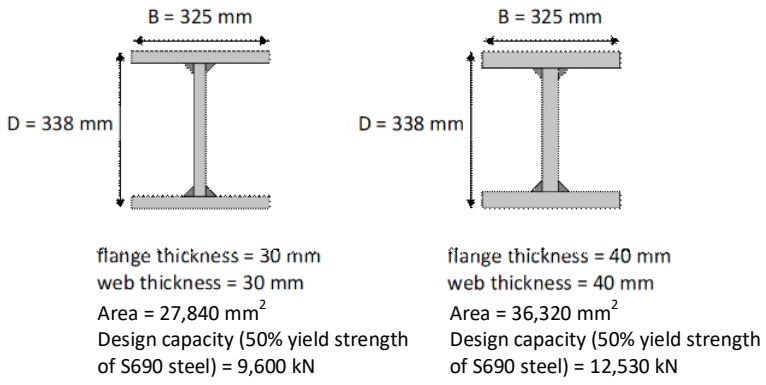
Figure 1.1: (left) Tseung Kwan O Cross Bay Link with S690 steel;
(right) Lung Yeuk Tau Interchange footbridge with S960 steel

1.1 Potential applications in pile foundations

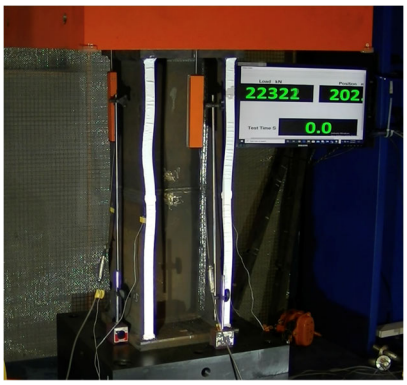
Besides the clear benefits in superstructures, the use of high-strength steel materials can potentially bring similar advantages in underground constructions, such as pile foundations. Pre-bored socketed H-pile is a common foundation option in Hong Kong. The construction process of these piles involves inserting steel H-sections into pre-bored holes supported by temporary steel casing, followed by injection of cementitious materials to fill the annular space between steel section and the borehole wall whilst the steel casing is being extracted. The structural performance and serviceability of these piles are therefore governed by material strengths of steel and the grout, the interfacial bond behaviour at steel-grout, grout-rock or grout-soil interfaces, and the end bearing capacity of the rock, although the latter is rarely relied upon in the local design practice.

Replacing the steel H-section with high-strength (S690) or ultra-high-strength (S960) steel increases the structural capacity of a pile. Currently, pre-bored socketed H-piles are usually

designed to reach capacities of around 6000 kN. With the use of S690 steel sections, the design capacity of a socketed H-pile (with typical dimensions shown in Figure 1.2a) can be increased to 9500 kN or even 12500 kN, assuming 50% utilisation of the yield strength of steel. A laboratory study conducted by PolyU has already demonstrated the enhanced structural capacity of such H-sections (e.g. Figure 1.2b). Enhanced pile capacities can lead to reduction in number of piles, thereby reducing the associated site handling, drilling and logistical costs of the project, as well as the carbon footprint.



(a)



(b)

Figure 1.2: (a) Examples of built-up steel H-sections for pile engineering applications (b) S690 H-section (with flange and web thickness of 30 mm) loaded to above 22,000 kN in PolyU laboratory

1.2 Pain points and study objectives

Several concerns related to the design and construction aspects of high-strength steel piles need to be addressed, before the benefits can be realized in routine foundation engineering practice (BD, 2023; 2024; GEO, 2006):

- The length of rock socket is controlled by the geotechnical capacity of rock, particularly its bond strength with grout. In the current practice, the rock socket length is designed to match the structural capacity of the pile. Under the earlier design code provisions, using high-strength steel requires a relatively long rock socket to provide sufficient rock-grout bonding.
- Unlike some superstructure components that can be prefabricated and assembled off-site, individual steel H-sections need to be spliced in situ to form a pile. Site welding of high-strength steel and subsequent compliance testing could be a concern, since there is limited experience in Hong Kong regarding site welding and a lack of guidance of welding compliance test of high-strength or ultra-high strength steel sections.

To address these concerns, three pre-bored socketed high-strength S690 steel piles were installed and tested at Fung Kong, in the northern parts of the New Territories. The tests were conducted with the following objectives:

- To investigate the geotechnical capacities of these piles, which are socketed into meta-sedimentary rocks prevalent in the region.
- To demonstrate the constructability of pre-bored socketed steel piles with new materials including ground-granulated blast-furnace slag (GGBS) grout and high-strength S690 steel, especially on aspects regarding site welding and its quality control.
- To apply other innovative technologies in pile engineering, including distributed fibre optics sensing technologies, bi-directional loading systems in pile tests, and explore the feasibility of robotic welding, etc.

2. Trial Piling Works in the Northern Metropolis

2.1 Overview of the pile loading test programme in the Northern Metropolis

The Northern Metropolis is largely underlain by meta-sedimentary (MS) rocks. Many of these rocks had been subject to folding, faulting, metamorphism and deep weathering. Owing to limited geotechnical information available at the time, conservative presumed design values were adopted for Category 2 MS rock in the Code of Practice for Foundations 2017 (BD 2024).

In view of the substantial development works planned in the region, GEO of CEDD initiated a large-scale pile loading test programme in 2023 under *Agreement No. CE 87/2022 (GE) Regional Geological Study of Northern New Territories (Northwest) – Feasibility Study*. The programme investigated the end-bearing and rock socket shaft resistance of piles founded in MS rock to support a review of the presumed allowable design values. It comprised test site selection, ground investigation, trial pile design, field monitoring and interpretation of the test results. Full-scale instrumented trial piles founded in MS rock were constructed across the Northern Metropolis (Figure 2.1). The programme has three main objectives, as described below.

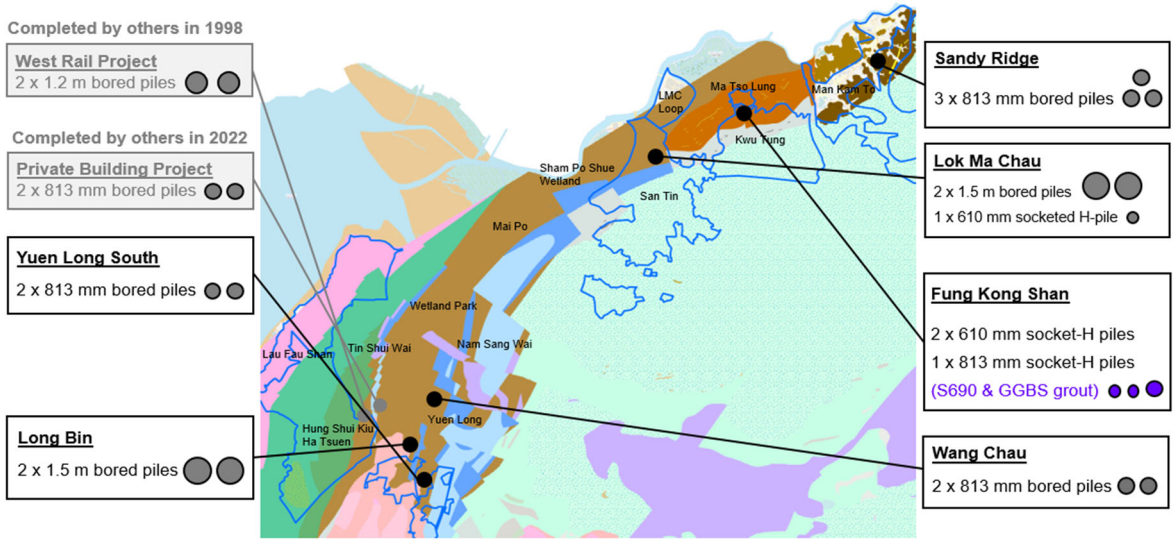


Figure 2.1: Locations of Trial Piles in Meta-sedimentary Rocks under the Pile Loading Test Programme in the Northern Metropolis

Investigation of Pile Performance in MS Rocks. The first objective is to collect field data on the end-bearing capacity and rock socket shaft resistance of piles founded in MS rocks. These data are used to review whether there is margin for enhancing the presumed design values in the *Code of Practice for Foundations 2017* (BD, 2024). Rock-socketed bored piles and socketed H-piles were tested using different loading configurations, including bi-directional static load tests using Osterberg cells (O-cells), static compression test with kentledge reaction; and multi-level bi-directional static load test using Y-Jacks. Strain gauges and distributed fibre optic sensors were installed to assess load transfer along the piles.

The results of the wider trial piling programme provided the technical basis for the revised allowable end-bearing and bond stress values promulgated in GEO TGN No. 53 (Issue 2) (GEO, 2026). This TGN promulgates the key outcome of the programme, translating full-scale field evidence into enhanced foundation design guidance for MS rocks.

Evaluation of the Use of GGBS in Concrete and Grout. The second objective is to evaluate the feasibility of using concrete and grout with a high replacement level of ground granulated

blast-furnace slag (GGBS) in pile construction. As a by-product of the iron manufacturing industry, GGBS has significantly lower embodied carbon than ordinary cement and offers considerable potential to reduce the carbon footprint of foundation works (Higgins, 2007). However, its use in piling works in Hong Kong has been limited by concerns over constructability and performance. Large-diameter bored piles with high GGBS replacement were therefore constructed and closely monitored, and a non-shrink grout with high GGBS replacement was adopted for the socketed H-piles. Key findings of the trial bored piles with high percentage GGBS concrete have been discussed by Chiu & Sze (2024).

Demonstration of the Application of High-strength steel in Pile Foundations. The third objective is to demonstrate that socketed H-piles with high-strength steel sections can be constructed on site and perform satisfactorily to meet the quality and load-taking requirements. Their wider use has been limited by conservative rock socket design values and limited local experience in the site welding of high-strength steel. In this study, the trial piles at Fung Kong were designed to demonstrate on-site welding, inspection and installation of socketed H-piles with high-strength steel sections. They were also designed to examine the interaction between the steel, grout and surrounding rock.

2.2 Trial piles using high-strength steel in Fung Kong

The Fung Kong test site (Figure 2.1) is located within the Northern Metropolis. Geologically, the region is underlain predominantly by meta-sedimentary (MS) rock, which comprises metamorphosed sandstone and carbonaceous siltstone with graphitic interbeds, commonly present as meta-siltstone and meta-sandstone (Figure 2.2). The engineering behaviour of MS rock is complicated by its inherent heterogeneity, fracturing and brecciation (Figure 2.3), which render its bearing capacity difficult to characterise reliably. As the deep foundations supporting many developments in Northern Metropolis will be founded largely within this stratum, the reliable determination of the load-carrying behaviour of piles socketed in MS rock constitutes a prerequisite for safe and economical foundation design across the region. The Fung Kong site is representative of these conditions, and the site forms one component of a territory-wide instrumented trial-piling programme undertaken across the northern New Territories. It also serves as a trial location for high strength Grade S690 socketed-H piles and GGBS grout.

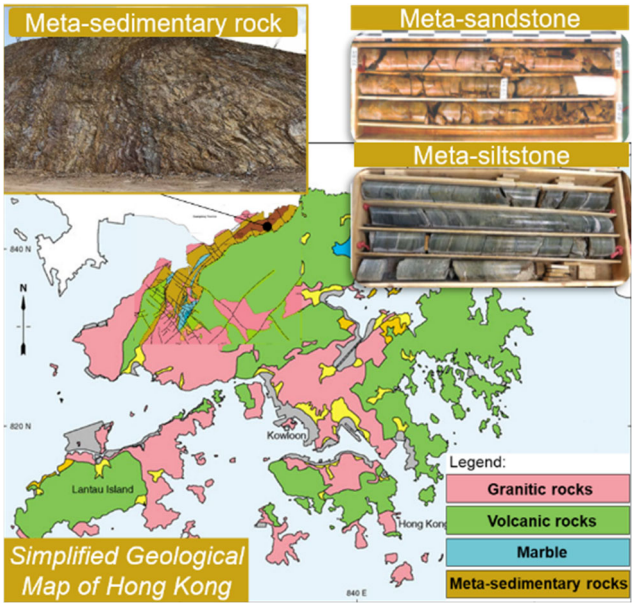


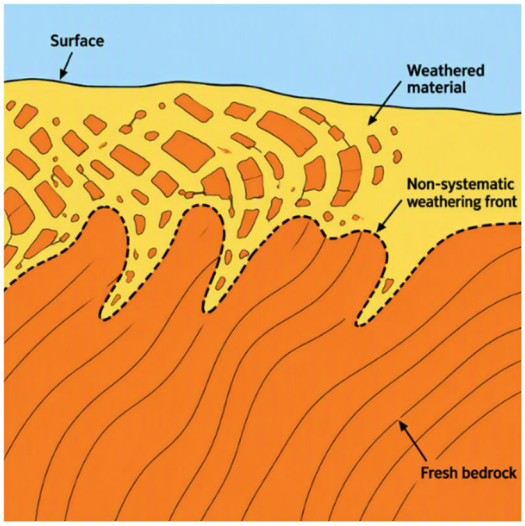
Figure 2.2: Simplified geological map showing the principal rock types of Hong Kong

The limited historical full-scale test data noted in Section 2.1 were reflected in the presumed allowable design values adopted for MS rock. Specifically, under the *Code of Practice for Foundations 2017* (BD, 2024), prior to this study, Category 2 MS rock is assigned a presumed allowable end-bearing pressure of 3,000 kPa, and presumed allowable bond friction between rock and concrete/grout of 300 kPa (under compression or transient tension) or 150 kPa (under permanent tension). These values are significantly lower than those allowed for igneous rock of comparable weathering grade and total core recovery. This disparity has direct implications for foundation economy, and even feasibility of certain pile types such as pre-bored socketed steel H-piles.

A review of overseas standards, including *British Code of Practice for Foundations (BSI, 2020),* the *AASHTO LRFD Bridge Design Specifications (AASHTO, 2007)* and the *Canadian Foundation Engineering Manual (CGS, 2006)*, indicates that no established guideline is specific to MS rock, and that meta-sedimentary rocks are generally assigned lower presumed bearing values than massive crystalline rocks. The characterisation of the allowable end-bearing pressure of MS rock is further complicated by its inherent heterogeneity, fracturing and brecciation associated with metamorphism, and non-systematic weathering profile (Figure 2.3). These considerations establish the need for field-verified design parameters derived from full-scale testing, and for their comparison against current publications of the Geotechnical Engineering Office and the Buildings Department.



(a)



(b)



(c)

Figure 2.3: Engineering Geological Issues with meta-sedimentary Rocks: (a) Silicification; (b) Non-systematic Weathering Profile; (c) Fractures and Brecciation

2.3 Site geology and ground investigation at Fung Kong

The three trial piles, SHP-FK-P1, SHP-FK-P2 and SHP-FK-P3 were positioned within a compact area, at existing ground levels ranging from +28.3 mPD to +30.7 mPD. The regional geology is derived from the 1:20,000-scale published Geological Map, Sheet 2 - San Tin (Figure 2.4, GEO 2022). The superficial deposit across the site is predominantly the colluvium of the Chek Lap Kok Formation (Qcd), comprising sand, gravel, cobbles and boulders in a silt matrix. The solid geology is recorded predominantly as grey to red fine sandstone, laminated siltstone and black carbonaceous mudstone of the Tai O Formation (Jo), which is also recorded to be mylonitised across the site. No faults or photogeological lineaments are recorded within 100 m of the site, the nearest fault being inferred approximately 150 m to the south. The meta-sedimentary bedrock at Fung Kong forms part of the wider Lok Ma Chau Formation sequence that predominates in the northern New Territories.

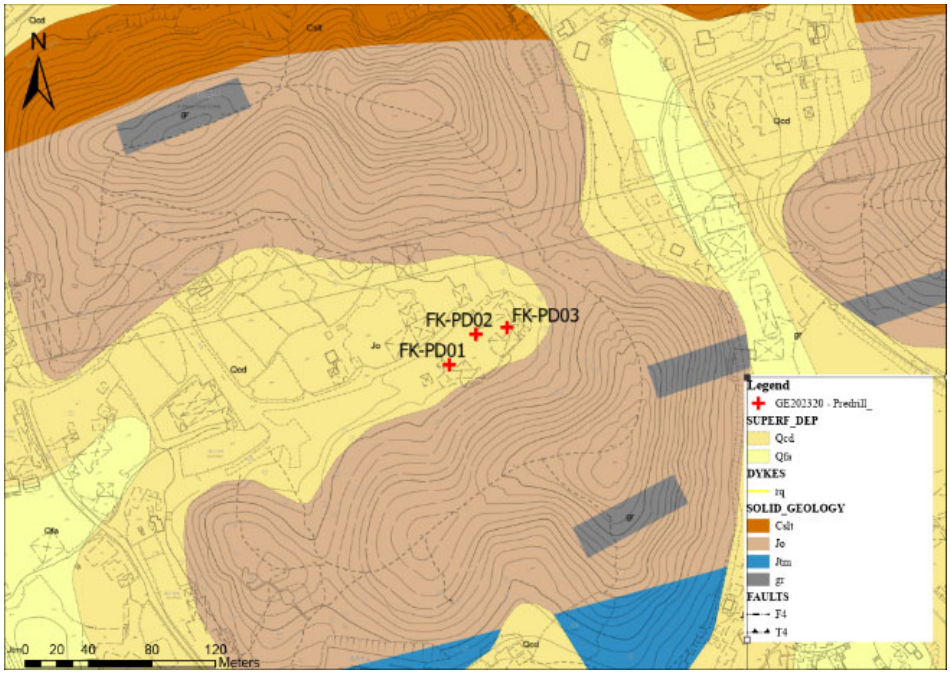
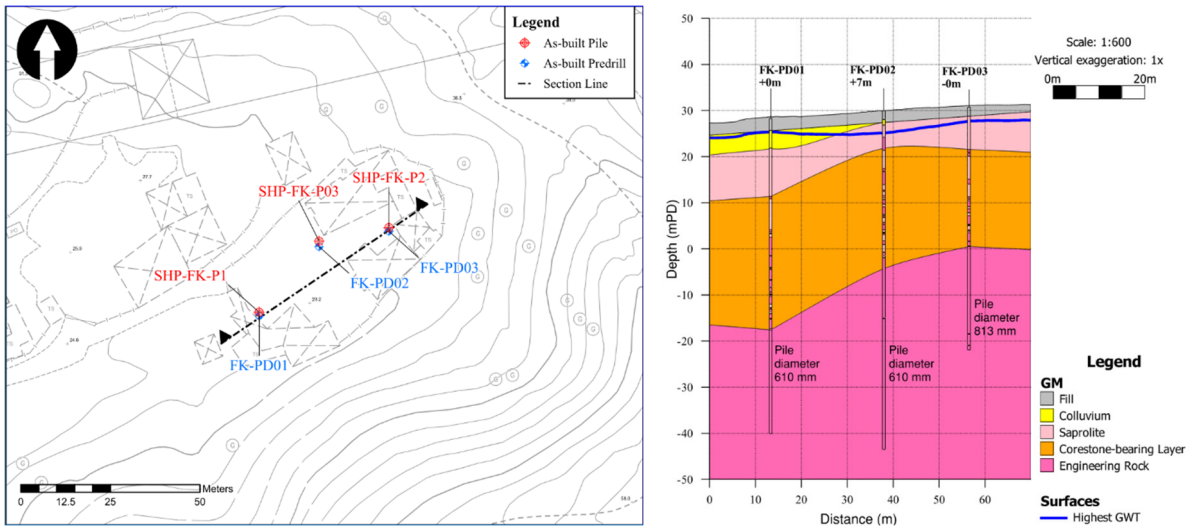


Figure 2.4: Hong Kong Geological Map, Sheet 2 - San Tin (GEO, 2022)

The ground conditions at each pile location were investigated by rotary-core predrilling prior to determining the founding level, using a skid-mounted drilling rig with double-tube barrels in the rock to maximise core recovery. Predrill boreholes FK-PD01, FK-PD02 and FK-PD03 (Figure 2.5) were advanced to represent SHP-FK-P1, SHP-FK-P3 and SHP-FK-P2 respectively. Core photographs from the three boreholes (Figure 2.6) show a broadly similar but laterally variable stratigraphy comprising fill, colluvium, a completely-to-highly decomposed saprolite, a zone of partially weathered rock of alternating decomposition grades, and the engineering rockhead. The variability characteristic of MS rock is reflected in the markedly different rockhead levels across the site. The founding stratum in each case is primarily grey, moderately strong to strong, moderately to slightly decomposed meta-siltstone and meta-sandstone. Standard penetration tests recorded refusal-level blow counts within the saprolite and partially weathered rock, confirming the dense, progressively less weathered profile with depth. The groundwater table was encountered at shallow depth, varying between approximately 2.9 m and 5.4 m below ground level across the boreholes.



(a) (b)

Figure 2.5: (a) Site Plan Showing the As-built Positions of the Trial Piles and Predrill Boreholes; (b) Interpreted Geological and Weathering Profile Along the Section

For piles founded in rock, the relevant design parameter is not governed by the strength of the intact rock alone, but by the features of rock mass surrounding and below the pile base. This is particularly important for meta-sedimentary (MS) rock, where bedding, joints, localised weak bands and variable weathering can control the deformation and load-transfer response, even where individual core specimens may appear strong. Rock mass characterisation therefore provides the link between ground investigation records and rational foundation design, allowing the founding stratum to be assessed in terms of both material strength and discontinuity-controlled mass behaviour.

GEO Publication No. 1/2006 (GEO 2006) provides an empirical basis for relating rock mass quality to allowable bearing pressure for foundations. The approach recognises that pile-base behaviour is influenced not only by intact rock strength, but also by rock quality designation (RQD), joint spacing, joint condition and groundwater condition. These factors are combined through the Rock Mass Rating (RMR) system of Bieniawski (1974), as adopted in GEO (2006), with the resulting RMR used to inform the selection of allowable bearing pressure over the relevant zone beneath the pile base.

For this study, laboratory and in-situ testing was used to support the rock mass assessment. For borehole FK-PD01 where SHP-FK-P1 was constructed, the RMR is approximately 45 within the socket and reduces to approximately 34 within $2D_s$ below the founding level, see also Figure 2.6(a).

For borehole FK-PD03, where SHP-FK-P2 was constructed, the RMR is approximately 45 within the socket and increases to about 58 within $2D_s$ below the founding level, as indicated in Figure 2.6(c).

For borehole FK-PD02, where SHP-FK-P3 was constructed, RMR ranges from 38 to 49 within the rock socket and is approximately 57 within a depth of 2Ds below the founding level, as shown in Figure 2.6(b). Overall, these values indicate modest rock mass quality for a rock-founded pile system, consistent with the heterogeneous nature of the meta-sedimentary rock encountered at the site.

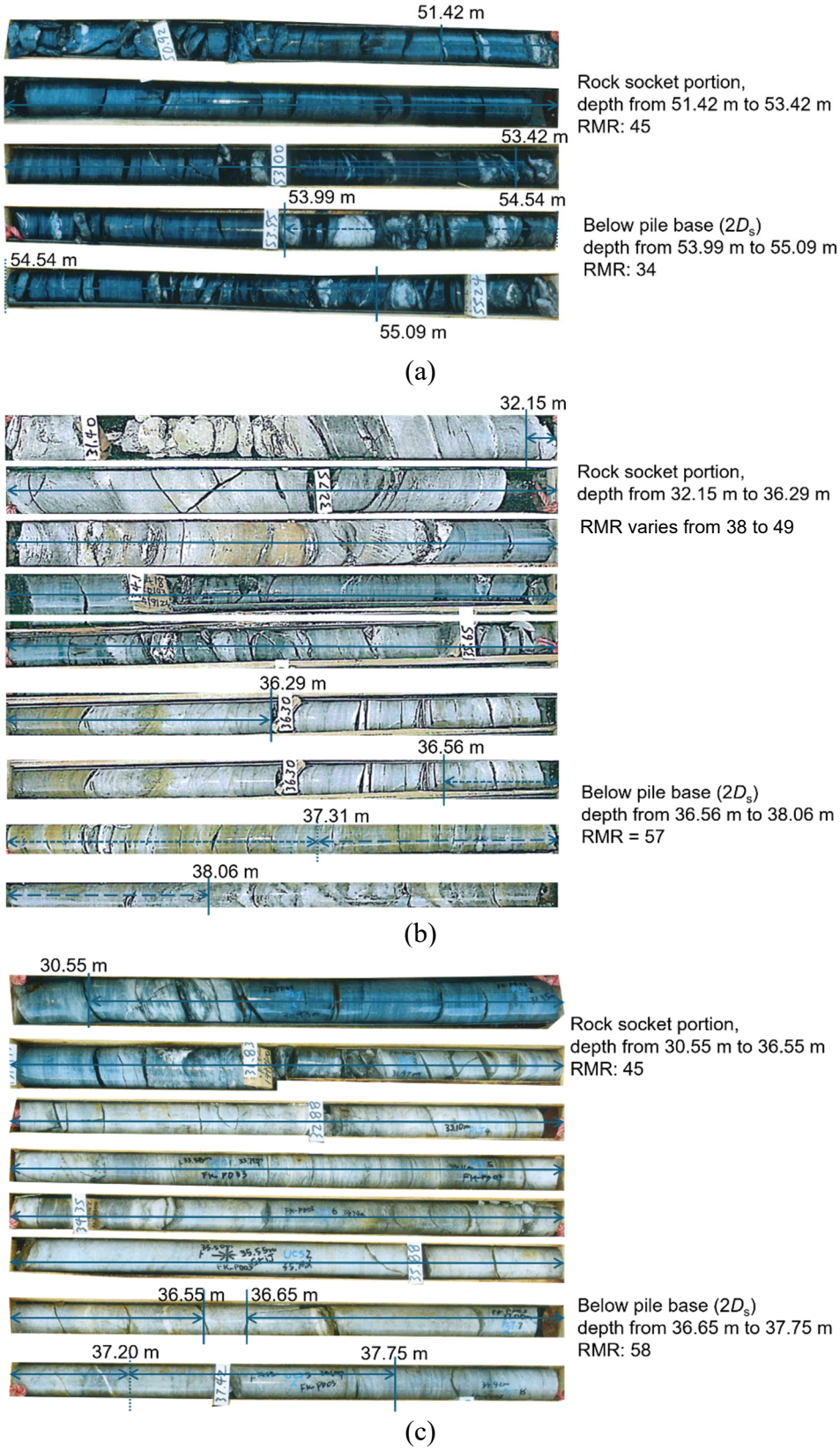


Figure 2.6: Photographs of Rock Cores Recovered from Predrill Boreholes (a) FK-PD01; (b) FK-PD02; and (c) FK-PD03

2.4 Design, construction and test arrangements of three trial piles

The Fung Kong programme constitutes the first coordinated dataset in Hong Kong in which the shaft friction and end-bearing behaviour of piles socketed in meta-sedimentary (MS) rock are characterised using three independent loading systems on a single site. Three full-scale trial piles (i.e., SHP-FK-P1, SHP-FK-P2 and SHP-FK-P3) were installed, and each subjected to a different loading configuration, specifically, Osterberg-cell (O-cell) bi-directional test (Figure 2.7a), conventional kentledge static test (Figure 2.7b), and multi-level Y-Jack bi-directional test (Figure 2.7c). Because the three piles were constructed within a common geological setting and adopted comparable pile sections and construction methods, the programme provides a useful basis for comparing how different loading systems can be used to interpret MS-rock pile behaviour. The site forms one node of the wider territory-wide trial-piling initiative undertaken across the Northern Metropolis under Contract GE/2023/20, and is distinguished as the location at which high strength S690 socketed-H piles and eco-friendly GGBS grout are trialled.

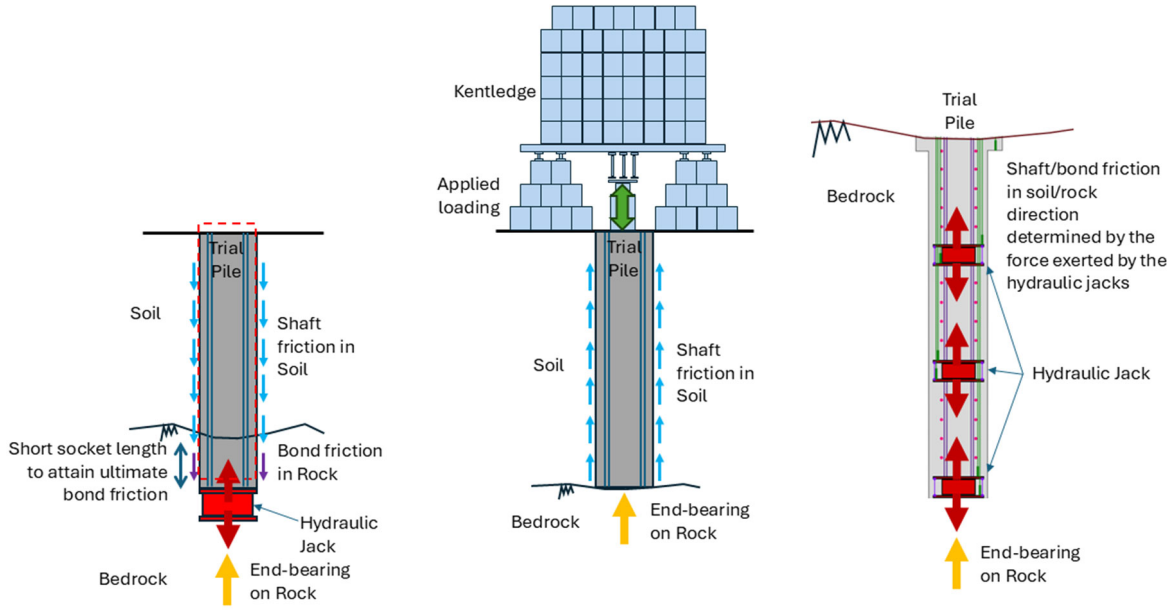


Figure 2.7: Working mechanisms of the three loading methods: (a) O-cell bi-directional Test; (b) Conventional kentledge static test; (c) Multi-level Y-jack bi-directional Test

The three loading systems adopted at Fung Kong all seek to quantify the shaft friction/bond at the rock socket and the end bearing at the pile base, but use different loading arrangements.

Both the O-cell and Y-Jack tests operate on the same bi-directional loading principle: hydraulic loading devices installed within the pile apply upward and downward forces simultaneously, with the resistance above and below the loading level providing mutual reaction. In this study, to meet the testing objectives, the O-cell test uses a single loading level near the pile base, whereas the Y-Jack test uses multiple loading levels within the rock socket.

In an O-cell bi-directional test (Figure 2.7a), a hydraulic cell is cast within the pile, usually near the base. When pressurised, the cell pushes upward and downward simultaneously. The upward force mobilises the rock socket shaft friction, and the downward force mobilises the end bearing. In this way, the shaft and base responses are measured independently in a single test.

The method is particularly efficient where the socket friction alone is sufficient to react the load required to prove the end bearing.

In a conventional kentledge (static) test (Figure 2.7b), load is applied at the pile head by hydraulic jacks reacting against a heavy kentledge platform placed above the pile. The applied load is resisted by the shaft friction along the pile and the end bearing at the base acting together. A full-size kentledge is required to provide a reaction at least equal to the maximum test load, which is costly and space-consuming for high-capacity piles. In this type of test, the shaft resistance can be isolated by installing a compressible soft toe at the pile base to suppress the end bearing.

The Y-Jack bi-directional test extends the single-cell test by installing several flat jacks at different levels within the rock socket (Figure 2.7c). Each jack, when pressurised while the others are locked, mobilises the resistance of the rock socket segment between adjacent jack levels. This allows the friction of individual socket segments and the end bearing to be isolated and measured separately within a single pile. This provides a far more detailed picture of load transfer than a single-cell test. A locked jack acts as an integral part of the pile and transmits load across itself, whereas a free jack transmits no load and thereby de-couples the resistance above and below it.

2.4.1 Design and construction of the trial piles

The three trial piles were designed to a common configuration, i.e., a Grade S690QL socketed steel H-pile grouted within a permanent steel casing, but were configured differently to suit their respective loading systems and test objectives. They were also constructed using a common methodology, which provides a consistent framework for interpreting the test results while allowing each pile to be configured for its specific loading arrangement. The pile construction procedures are outlined below:

Excavation (Figure 2.8a): Each pile was formed using a drilling rig equipped with a Down-the-Hole hammer, with drilling advanced inside a steel casing to the base of the rock socket. The casing was retained as a permanent liner to stabilise the bore and reduce the contribution of soil shaft friction during testing, thereby allowing the applied loads to be transferred predominantly to the rock socket. The sockets were advanced into Grade III or better meta-sedimentary rock to provide a suitably competent founding material for the trial piles.

Sensor Installation (Figure 2.8b): The instrumentation was mounted on the H-section prior to installation. Paired strain gauges were fixed at multiple levels, which are closely spaced within the rock socket and more widely along the cased shaft, together with rod extensometers for displacement measurement, transducers for the O-cell or Y-Jack expansion, and distributed fibre-optic sensors for high-resolution strain profiles.

H-pile Installation (Figure 2.8c): Each pile used a Grade S690QL built-up steel H-pile. The flange-to-web welds were executed by automatic gas metal arc welding (GMAW) under a certified procedure, supervised by qualified S690 welders and inspected by an HOKLAS-accredited laboratory. The completed H-section, with its pre-mounted instrumentation, was then lowered into the cased bore to the founding level.

Grouting (Figure 2.8d): The rock socket and casing annulus were grouted in a single continuous operation by tremie, following final air lifting and verification of bore cleanliness. A non-shrink GGBS grout with a specified 28-day cube compressive strength of 30 MPa was used for all three piles, with the achieved strength exceeding this requirement.

The three test piles were designed to incorporate different detailing at the base or within the socket to serve different test objectives. For the test pile SHP-FK-P1, the 430 mm O-cell was installed near the pile base between two 50 mm thick, 474 mm diameter steel bearing plates. A short 100 mm length of H-section was extended beneath the assembly to transmit the downward O-cell load uniformly to the founding rock at pile-base level. For the test pile SHP-FK-P2, a 100 mm thick polystyrene soft toe was attached beneath the H-pile base to suppress the end-bearing contribution (Figure 2.8e), ensuring that the head-applied load was resisted predominantly by the rock socket bond friction. For the test pile SHP-FK-P3, an enlarged 750 mm diameter rock socket was adopted to house three Y-Jack flat-jack assemblies (each with 610 mm diameter, 70 mm thick bearing plates) at three levels, together with the dense strain-gauge instrumentation between them. The lowest jack (Y3) was pre-expanded by 25 mm prior to grouting to provide free movement at the pile base when the segment friction was subsequently isolated.



Figure 2.8: Construction Procedures for Trial Piles: (a) Excavation; (b) Sensor Installation; (c) H-pile Installation; (d) Grouting; (e) Polystyrene Soft Toe for SHP-FK-P2

2.4.2 Instrumentation

A consistent instrumentation system was adopted across the three trial piles to enable consistent interpretation of load-transfer mechanisms. The instrumentation arrangement for each pile is described below.

The trial pile SHP-FK-P1 was instrumented with 27 levels of paired vibrating-wire strain gauges (Figure 2.9a) installed on the H-section above the O-cell, extending from the cased shaft down to 0.3 m above the pile base. The gauges were closely spaced within the rock socket to capture the rapid attenuation of axial load in that zone, and more widely spaced along the upper cased shaft. Each level carried two gauges for cross-checking. Vertical displacements were monitored using three sets of paired telltale rods (Figure 2.9b), referenced to the rock socket top, the O-cell top plate and the O-cell bottom plate, and read by linear vibrating-wire displacement transducers (LVWDTs, Figure 2.9c) at the pile head. A further four LVWDTs positioned between the O-cell plates measured the expansion of the cell, and pile-head movement was independently monitored by a pair of automated digital survey levels. In addition, distributed fibre optic sensors (Figure 2.9d) were bonded to the steel section and embedded in the grout to provide high-resolution axial-strain profiles, which also served to verify the composite behaviour of the steel section and surrounding grout. Details of fibre optic sensing technologies will be elaborated in the Section 3.4.

The trial pile SHP-FK-P2 was instrumented with 16 levels of paired vibrating-wire strain gauges (Figure 2.9a), installed from 0.3 m below existing ground level down to 0.3 m above the pile base. The majority of the gauges were concentrated within the 6.07 m rock socket, at close vertical spacing, to document the load transfer along the socket, with only a few gauges positioned along the upper cased shaft. As with SHP-FK-P1, each level carried two gauges for cross-checking. Pile-head displacement was monitored by four dial gauges mounted against independent reference beams on both sides of the pile, supplemented by periodic survey checks. As for SHP-FK-P1, distributed fibre-optic sensors were bonded to the steel section and embedded in the grout to provide high-resolution axial-strain profiles.

The trial pile SHP-FK-P3 was instrumented with 23 levels of paired vibrating-wire strain gauges (Figure 2.9a). In the cased shaft the gauges were spaced at approximately 4 m intervals, whereas within the rock socket they were installed at a maximum vertical spacing of only 240 mm between the three jack levels, providing high-resolution load-transfer data within each of the three socket segments. Vertical displacements were monitored using eight sets of paired rod extensometers (Figure 2.9b), referenced to the pile head, the rock socket top, and the top and bottom plates of each of the three Y-Jacks, and read by electronic displacement transducers fixed to a reference beam at pile-head level. This arrangement was necessary to capture the movement of each jack independently. Fibre-optic sensors (Figure 2.9d) were embedded in the grout to provide continuous strain profiles.



Figure 2.9: (a) Strain gauge; (b) Extensometer; (c) LVWDT; (d) Optical fibre

3. Innovative applications in Fung Kong test piles

3.1 High-strength steel in construction

In this document, the terms 'high-strength' steel or 'ultra-high strength' steel refer to steel materials with minimum yield strengths exceeding 690 MPa and 960 MPa, respectively, which are significantly higher than 'normal grade' steel of yield strengths of 355 MPa or 460 MPa (or lower) (Figure 3.1). Advanced steel manufacture technology had emerged in the 1990s, and steels with such high strengths were produced in European countries and Japan. Initially, high-strength steel materials were produced as plates with thickness ranging from 6 to 30 mm, and the major areas of application were confined to machinery and lifting equipment in ports or mines, etc. The high costs associated with the production of such materials had previously resulted in the lack of applications in construction. For many years, the costs of high-strength steels were at least 1.7 to 2.5 times that of S355 steel. Hence, there was no financial incentive to adopt them in the construction industry, which often entails large amounts of steel in each project.

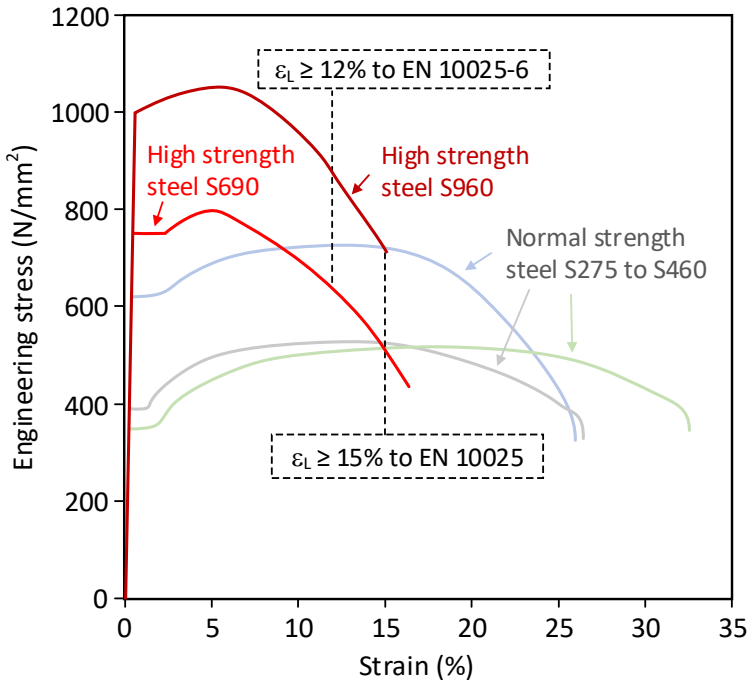


Figure 3.1: Typical stress-strain response of high-strength steel and normal grade steel (after Chung, 2022)

Since the 2010s, significant leaps have been made in the steel manufacturing technology in China. The leading Chinese steel producers now possess the capabilities to regularly produce high-strength and ultra-high strength steel plates of thickness ranging from 6 to 80 mm. These high-strength steels are manufactured with specific compositions of special metallic elements through well-controlled heat treatments known as quenching and tempering. The processes produce fine-grained crystals that give rise to the high strength and toughness, and hence excellent mechanical properties of the steel. In the context of adoption in construction industry, the game-changer is the cost of high-strength steel production in China. In recent years, the unit cost of S690 steel materials has been lowered to around 1.25 to 1.35 times that of normal grade steel. Apart from direct saving on material costs, reduced steel tonnage generally leads to reduced efforts on fabrication, logistical costs, and in the case of steel superstructure, smaller loads onto the foundations and hence the associated costs can also be reduced.

While the reduced production costs cleared a major hurdle for its application in construction, another challenge lies on the potential changes in properties of high-strength steel subjected to welding. As mentioned earlier, the enhanced strength of such steels arises from the fine-grained crystals that form during the manufacturing process. If the heat input energy during welding and cooling rates after welding are not properly controlled, the ensuing heating-cooling cycles may initiate phase transformation and re-crystallisation and grain growth in the microstructures of welded sections, which eventually lead to subpar performance of the steel elements.

Extensive research has been conducted at PolyU (Figure 3.2) to investigate the thermo-mechanical properties of high-strength steel and the welded sections. These include experimental study and numerical simulations to understand the temperature distributions during welding and residual stresses after welding. These enabled the development of practical welding procedures that minimise or even eliminate strength reductions at welded sections of high-strength steel. Quality assurance measures were also established based on the scientific knowledge, to provide practical guidance for frontline construction staff, design engineers and regulatory agents. Robotic welding systems were also established to set the benchmark for improved welding quality and repeatability. With the support and collaboration with various stakeholders of the steel manufacturing and fabrication community, the sustained research efforts eventually led to site deployment of robotic welding apparatus, and also the training and certification of qualified welders and robotic welding operators. These various aspects all contributed to the successful field trial of socketed S690 high-strength steel piles at Fung Kong, which will be elaborated in subsequent sections.



Figure 3.2: Testing of S690 and S960 steel H-sections at PolyU

3.1.1 Site welding of high-strength steel piles

The Fung Kong test piles utilised S690 high-strength steel sections, with the key advantage of enhanced pile capacities which may lead to reduced number of piles compared to foundation design with normal grade steel piles. Besides, socketed high strength S690 (or S960) steel piles can reach capacities that are comparable to some concrete bored pile designs, yet they require

less heavy construction equipment compared with bored piles. However, the length of socketed H-piles are governed by local geology, particularly the depth to bedrock stratum. In many cases, this means that it is necessary to splice individual H-sections on site by welding.

While site welding for normal grade steel works has been a routine practice in Hong Kong, this is less common for high-strength steel such as S690 and S960. Considering that site welding is almost inevitable for steel piling works, it is essential that their constructability and quality control measures could be demonstrated in the full-scale field trials.

3.1.2 Importance of welding procedures from metallurgical perspective

High-strength steel gains its enhanced properties through carefully-controlled quenching and tempering processes that produce fine-grained microstructures in steel. These materials are sensitive to thermal input during welding operations. Poorly-controlled welding operation introduces heat cycles that degrade the fine-grained microstructure within the heat-affected zone (HAZ). The major risks associated with the HAZ include microstructural softening and grain coarsening, which refers to the phase transformations and grain growth caused by excessive heat inputs. These lead to localized reductions in yield strength, ultimate strength, and ductility of the high-strength steel. Meanwhile, rapid and uneven cooling in the presence of residual moisture promotes hydrogen-induced delayed cracking, which is associated with the formation of brittle structures susceptible to cold cracking under internal restraint. Moreover, weld shrinkage introduces high locked-in stresses that can range from 30% to even 100% of the nominal yield strength. These severely compromise the structural performance, especially the buckling resistance of the elements.

The Chinese National Engineering Research Centre (CNERC) for Steel Construction (Hong Kong Branch) of PolyU has conducted an extensive series of research studies since the early 2010s (Figure 3.3). These included simulated HAZ thermal cycles and physical testing to establish welding parameters to ensure the quality of welded connections involving high-strength steel materials of different connected thicknesses. A comprehensive quality assurance framework was established, combining Non-Destructive Testing (NDT) for detection of surface and volumetric defects, with Destructive Testing (DT) for mechanical performance. The DT regime included (i) tensile tests for mechanical strength, (ii) bend tests for ductility and bendability of welded joints, (iii) Charpy impact tests to verify impact toughness under specific working temperature conditions, and hardness tests restricted to below 420 HV to control hydrogen cracking risk and ductility reduction after welding-induced heat cycles. Besides, through the extensive experimental study by PolyU CNERC on welding-induced residual stresses and their influence on member buckling under compression and bending, it is confirmed that the existing Eurocode buckling curves remain valid for high-strength steel sections. These findings also supported updates to the 2023 Hong Kong Steel Code and submissions to the European Committee for Standardisation (EC3).

The research on welding parameters and effects on microstructure led to the development of Welding Procedure Specifications (WPS) for high-strength steel applications, and Welding Procedure Qualification Tests (WPQT) that have been approved by HOKLAS-accredited laboratories. A typical set of welding procedures for S690 high-strength steel sections for H-pile applications is shown as an example in Table 3.1.

Table 3.1: Key parameters of welding procedure specifications for Grade S690J0 UBP.

1. Plant – 400Amp, 346 Volts as weld set.
2. Electrode of Shielded Metal Arc Welding –
   - Welding Electrode to AWS A5.5 E11016-G (e,g, Kobe Steel LB-116) – The strength level must be adapted to Grade S690J0.
   - Diameter range: 3.2 to 5 mm
   - Consumables including electrodes shall be kept and handled in a controlled manner in accordance with BS EN 1011-1. Any drying or baking of electrodes before issue shall be carried out in accordance with the recommendation of the manufacturer.
3. Joint preparation – beveling by manual flame cutting.
4. Joint type – Single bevel (45^{o}) with backing. The gap should be ranging from 2 ~ 4mm.
5. The design run length & run out ratio should comply with BS EN ISO 2560:2009. For 4mm diameter of electrode, the maximum run length & run out ratio to be 235m & 0.58 respectively.
6. Weld metal build up –
   - Electrode of 4mm diameter is for root layer, while Electrode of 5mm diameter is for subsequent layers.
   - Inter run cleaning –
     Each run of weld meter should be thoroughly cleaned by hand tools before a further layer is applied.
7. Preheating procedures and requirements shall comply with the manufacturer's recommendations, BS EN 1011-1:2009, and the qualified welding procedure specification (WPS) evaluated in accordance with BS EN ISO 15614-1:2017+A1:2019.
8. Heat input control shall be performed throughout the welding process. The maximum allowable heat input is limited to 1.5 kJ/mm for joint thicknesses less than 50mm and 2.0 kJ/mm for joint thicknesses greater than or equal to 50mm. The welding parameter including voltage (U), current (I), and travelling speed (v) shall be evaluated by the following formula:

   Line heat input energy, $q = 0.85\ U\ I\ /\ v$

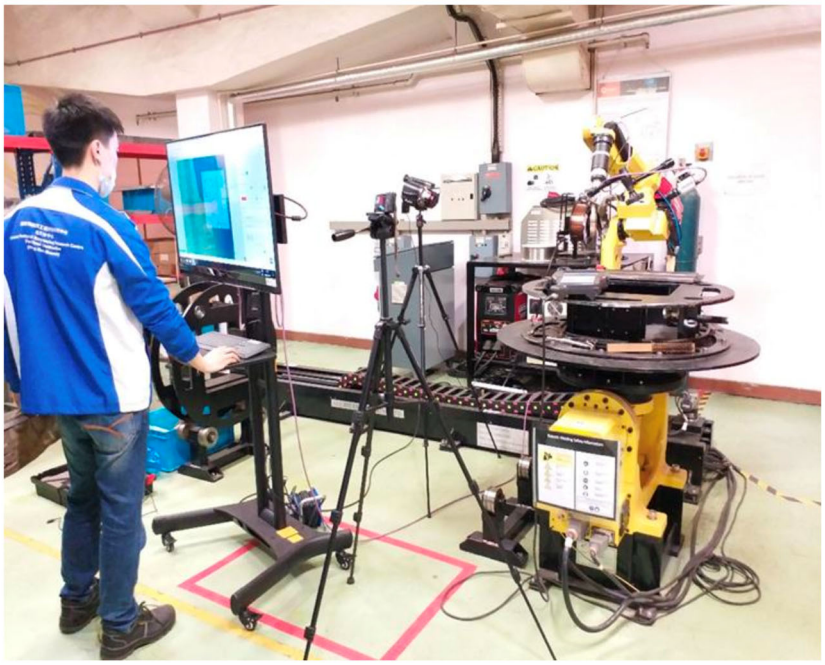


Figure 3.3: Robotic welding system at PolyU CNERC

3.1.3 Comparing welding procedures of S690 steel and normal grade steel

Welding high strength structural steel, such as S690, presents distinct metallurgical and procedural challenges compared to standard structural grades. Higher yield strengths necessitate stricter process parameters to preserve toughness, prevent HAZ degradation and avoid severe cracking phenomena. The specific features of welding processes are compared in four aspects:

(i) Selection of filler materials and hydrogen control

The choice of welding consumable is fundamental when joining high-strength steels. Standard carbon-manganese filler metals, such as ISO 14341-A G 42 2 C1 3Si1 used for S355, are unsuited for high-strength steel applications. S690 requires micro-alloyed consumables such as EN ISO 18276-A-T 69 6 Mn2.5Ni M M 3 H5, which supply higher nickel and manganese levels to ensure adequate tensile strength and sub-zero impact resistance. Filler metal selection dictates the diffusible hydrogen content in the weld deposit. The "H5" designation ensures diffusible hydrogen remains under 5 mL per 100g of deposited metal, which is vital for preventing hydrogen-assisted cold cracking (HACC).

(ii) Preheating, interpass, and post-weld heat treatment (PWHT)

Preheating and post-weld heat treatment routines are governed by chemical compositions of the base metal and the selected filler metal. Compliance with BS EN 1011 (*Welding — Recommendations for welding of metallic materials*) is essential to determine accurate thermal limits based on carbon equivalent values and hydrogen scales.

For example, for equivalent tension joints of S355 and S690, both procedures mandate a minimum preheat temperature of 20°C, a maximum interpass temperature capped at 160°C, and omit post-heat treatment. However, strictly maintaining the maximum interpass temperature is much more critical for S690. Exceeding 160°C in high-strength steels leads to excessively slow cooling rates, which coarsen the grain structure and drastically degrade yield strength and impact energy in the HAZ.

(iii) Heat input and run sequence

Controlling heat input is critical when welding quenched and tempered steels like S690. To preserve mechanical properties, S690 demands a lower heat input (~1.2 kJ/mm) compared to S355 (~1.5 kJ/mm). Consequently, achieving an equivalent joint geometry in S690 requires a finer, multi-run technique. This multi-pass deposition refines prior weld passes through thermal cycling, improving overall joint ductility.

(iv) Quality Assurance and Compliance NDT Hold Times

Because high-strength steels are susceptible to delayed hydrogen cracking—where defects form hours or days after cooling—quality control procedures must enforce mandatory holding periods prior to final inspection. Non-Destructive Testing (NDT) for S355 requires a hold time of 15 hours. In contrast, compliance testing for S690 requires an extended 40-hour hold time before performing NDT, ensuring any latent hydrogen-induced defects are reliably detected.

3.1.4 Robotic welding and process control

When properly set up, robotic site welding provided stable parameter control, consistent heat input and proper torch and arc alignment, ensuring the preservation of qualified metallurgical conditions. On the other hand, small deviations in joint preparation can alter the arc length and quality of heat input control, cause mismatches between programmed and actual torch paths, and compromise defect detection performance. To ensure dimensional tolerance placement and prevent movement, precise jigs, fixtures, and strongbacks can be utilized along with careful joint preparation prior to welding. In addition, proper operational awareness and execution of preheating processes utilizing either flame torches or digitally controlled heating elements were implemented as essential hardware controls to maintain process integrity.

Following welding completion (either by manual or robotic welding), post-weld heat treatment should be maintained using conventional insulation, such as rock wool held in place with appropriate brackets, to control cooling in accordance with the qualified WPS.

3.1.5 Training of welders and robotic welding operators

To address the demands of the industry on qualified and skilled welders for construction projects involving high-strength steel, PolyU CNERC has been collaborating with the Construction Industry Council (CIC) since 2023, to provide training to ‘upskill’ welders for high-strength steel welding operations (Figure 3.4). As of 2026, more than 60 welders have passed the relevant training and are qualified for site welding of S690 and S960 steel members.

Meanwhile, robotic welding amplifies the need for rigorous quality assurance. A dedicated operator qualification framework was instituted in mid-2025, in compliance with relevant EN ISO standards and WPS protocols. In the training programme, welders underwent structured upskilling that covered knowledge in high-strength steel metallurgy, robotic programming and motion control, operational safety, troubleshooting, and quality inspection techniques, with hands-on training to perform robotic welds that followed qualified WPS and subsequently subjected to full NDT and DT requirements to confirm compliance. The first cohort of 38 personnel was certified in October 2025. With support by industry parties and CIC funding, the programme targets over 200 certified robotic welding operators and trainers to address the needs of the construction industry.



Figure 3.4: On site welder training for high-strength steel welding (at another project site)

Commissioned by CEDD and in collaboration with PolyU, the Building Technology Research Institute (BTRi) published Hong Kong's first Technical Guidelines for Robotic Welding Operations of Structural Steel in Construction in early 2026 (CEDD and BTRi, 2026). The guidelines outline the essential knowledge for robotic welding operators, and the key requirements of robotic systems for structural welding on several aspects such as positional and repeatability accuracy, load capacity, durability and fatigue resistance, range of motion, etc.

At the Fung Kong test site, while on-site robotic welding is feasible, qualified welders were engaged to perform the splicing of H-sections during the pile installation process. Pre-heating and other welding procedures followed the WPS for high-strength steel applications, and the welding process took less than 2 hours for each splice. All necessary requirements for weld inspection were also satisfied.

3.2 GGBS grout in pre-bored socketed H-piles

The use of low-carbon supplementary cementitious materials to replace cement in the grout or concrete mix has received widespread attention in research and is being gradually applied in the industry. For example, GGBS has been identified as a potential replacement for cement. GGBS is obtained from the blast-furnace of steel mills by quenching the molten slag in water, resulting in granulated particles with higher fineness than ordinary Portland cement. Major structures in Chinese Mainland, including the Three Gorges Dam, Beijing-Shanghai Express Rail and major suspension bridges have involved the use of GGBS in the concrete, with replacement levels of around 40%. In Hong Kong, major infrastructure projects including the Tsing Ma Bridge and Stonecutter Island Bridge also adopted GGBS-based concrete with replacement levels of around 60% (GEO, 2011). The General Specification for Civil Engineering Works (GS) specified that for public works projects in Hong Kong, GGBS can replace up to 75% of cement for normal concrete. They offer a more effective solution to minimize cement consumption compared to other supplementary cementitious materials like Pulverized Fuel Ash (PFA), which typically replaces up to 35% of cement.

Higgins (2007) reported that the manufacture of one tonne of Portland cement would require about 1.5 tonnes of mineral extractions together with 5000 MJ of energy, generating about 0.95 tonne of CO_2 equivalent in the process. On the other hand, as GGBS is a by-product of the iron manufacturing industry, the production of one tonne of GGBS would only generate about 0.07 tonne of CO_2 equivalent and consume about 1300 MJ of energy. This demonstrates clear

benefits in terms of sustainability and reduction of carbon footprint. It is expected that similar environmental benefits would prevail for GGBS-based grout material in foundation engineering, but its workability and practicality on site, as well as the mechanical aspects under shearing action and load transfer in socketed H-piles warrant in-depth systematic investigation.

3.2.1 Lessons learned from GGBS concrete bored piles

Prior to the design and installation of socketed S690 steel H-piles, the use of GGBS concrete in bored piles was investigated at other test sites of the trial pile programme as reported by Chiu & Sze (2024). The workability, durability and strength characteristics of GGBS concrete mixes were first tested in a series of laboratory and plant trials. Subsequently, trial bored piles with diameters up to 3 m were cast with GGBS concrete, with replacement levels up to 80% of the total cementitious contents. The temperature changes in these concrete piles were measured by extensive instrumentation, and slump tests, cube tests, crosshole tests and core tests were also performed to assess the various aspects of feasibility considerations in adopting GGBS concrete in piles.

The test results indicated generally lower early strength developments in GGBS concrete with high replacement levels, which matched with the temperature change patterns in the piles. Still, the compressive strength requirements were successfully achieved. The workability and slump retention both met design specifications. Compared with PFA concrete, GGBS concrete displayed higher adhesiveness, but there were no significant issues that arose on site during the tremie concreting or casing extraction processes. The thermal monitoring results revealed lower peak heat generation with increased GGBS contents, which also reduced risks of thermal cracking in the concrete piles.

3.2.2 GGBS grout mix at Fung Kong test site

To evaluate the feasibility and in situ performance of GGBS grout in pre-bored socketed steel H-piles, laboratory and plant trials have been performed to test and refine the grout mix, followed by its field adoption and performance assessments in the subsequent load tests of three socketed S690 high-strength steel piles. The key design criteria of the GGBS grout included a minimum characteristic 28-day cube compressive strength of 30 MPa, and maximum bleeding limit of 2% within the first 3 hours after mixing, with total bleeding less than 4%. The bleeding and fluidity tests were conducted according to the relevant EN or ASTM methods for laboratory test, plant trials or site test, respectively.

Two sets of laboratory and plants trials were conducted on the grout mix with GGBS replacement levels of 60%, 70%, 75%, 80% and 85% (Figure 3.5 and Figure 3.6). The laboratory trial focused on evaluating the fundamental properties of the grout, including workability, strength and durability under controlled conditions; the plant trials allowed for the assessment of the mixes under a full-scale production condition, ensuring consistency and quality in real practice by the proposed plants. Based on test results in the first plant trial, it was observed that higher GGBS replacement ratios led to reduced bleeding in the cement grout. This trend may be attributed to the higher fineness of GGBS particles compared to ordinary Portland cement, which enhanced the overall fineness of the cementitious blend. This resulted in increased surface area and improved particle packing, which could promote better water retention and result in a more cohesive and stable suspension with reduced segregation and bleeding. The first set of plant trials also highlighted the importance of careful mix optimization to ensure that all strength, workability and flowability criteria could be met, and consistent performance could be achieved in field applications.

The second set of laboratory and plant trials facilitated modifications in the combination and dosages of additives such as set-retarding admixture, water-reducing agents and specialised bleeding control agent designed for non-shrink grouts, to optimize and balance the various aspects of grout performance. Comparisons between the test results from laboratory and plant trials also revealed the impacts of superior mixing efficiency achieved in the full-scale plant environment on the grout behaviour, both in terms of improved strength developments and bleeding performance. In particular, the prolonged high-shear mixing and more effective dispersion of superplasticiser and viscosity-modifying agents in the plant mixer delayed the onset of sedimentation, and reduced the rate of bleed water migration in the fresh grout. These observations further underscored the importance of plant-scale production in achieving optimal stability for high-volume GGBS grout systems.

Following the comprehensive study on the grout performance, the 30MPa non-shrink cement grout with 75% GGBS replacement was adopted for the socketed S690 steel H-piles at the Fung Kong test site. Details of the adopted GGBS grout mix are shown in Table 3.2. Three socketed steel H-piles were successfully constructed with the GGBS grout, confirming satisfactory constructability and placement characteristics under site conditions. While the cube strengths of GGBS grout have been proven satisfactory, the behaviour of the grouted piles under the load tests will be demonstrated in the subsequent sections.



Figure 3.5: GGBS grout samples in plant trial



Figure 3.6: Tremie grouting of trial pile

Table 3.2: Mix proportion of GGBS grout adopted for trial pile

Constituent	**Quantity per cubic meter of GGBS grout**
Total cementitious	1,340 kg
Cement	335 kg
GGBS	1,005 kg
Water	502 kg
Admixture KFDN-115G	5.00 litres
Admixture KFDN-SP2800	5.08 litres
Admixture KFDN-PPA800SX	31.40 litres
Water to cement ratio	0.37

3.3 Multiple pile testing methods

As mentioned in Section 2.4, the Fung Kong pile test programme is the first project site in Hong Kong in which socketed H-piles in meta-sedimentary (MS) rock are tested using three independent loading systems. The details of the test setup and loading procedures are elaborated in this section.

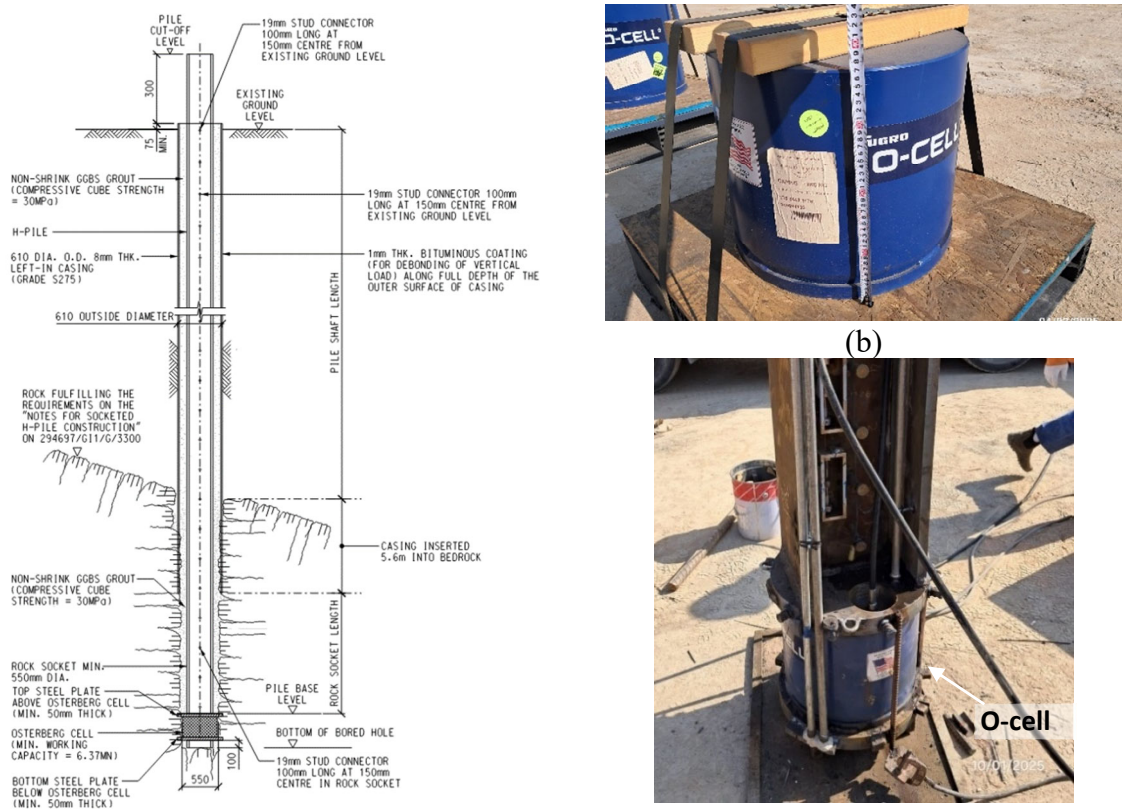
3.3.1 Test arrangement and loading procedures

***SHP-FK-P1*:** The arrangement of trial pile SHP-FK-P1 is shown in Figure 3.7. The pile was tested using an O-cell installed close to the pile base within a relatively short rock socket, allowing the rock socket resistance and pile-base response to be mobilised bi-directionally within the pile rather than through an external reaction system. This provided a compact means of applying high test loads to a socketed H-pile founded in meta-sedimentary (MS) rock, while enabling separate interpretation of the upward shaft resistance and downward end-bearing response. The O-cell was installed between steel bearing plates, with local detailing beneath the cell to distribute the downward load to the founding rock. Before the main loading sequence, a preliminary cycle was carried out to release the cell for testing and establish baseline readings. The test then proceeded through a series of loading cycles, including a sustained load-holding stage and a final cycle to explore the available cell capacity. The loading configuration and key load stages are summarised in Table 3.3.

***SHP-FK-P2*:** The arrangement of trial pile SHP-FK-P2 is shown in Figure 3.8. Unlike SHP-FK-P1, which adopted a bi-directional O-cell system, SHP-FK-P2 was tested using a conventional maintained-load kentledge arrangement, with load applied at the pile head through hydraulic jacks reacting against a kentledge platform. The pile incorporated a longer rock socket and was included to provide a conventional benchmark against which the bi-directional methods could be compared. A compressible soft toe was installed beneath the pile base to minimise the end-bearing contribution, so that the measured response would predominantly reflect load transfer along the rock socket. Load was applied incrementally and held at each load level, with pile-head settlement monitored against independent reference beams. The test comprised two loading cycles, including a sustained load-holding stage at the maximum test load, as summarised in Table 3.3. This configuration allowed rock socket bond behaviour to be assessed using the typical local testing method, while also providing a useful comparison with the more innovative O-cell and Y-Jack arrangements adopted in the same programme.

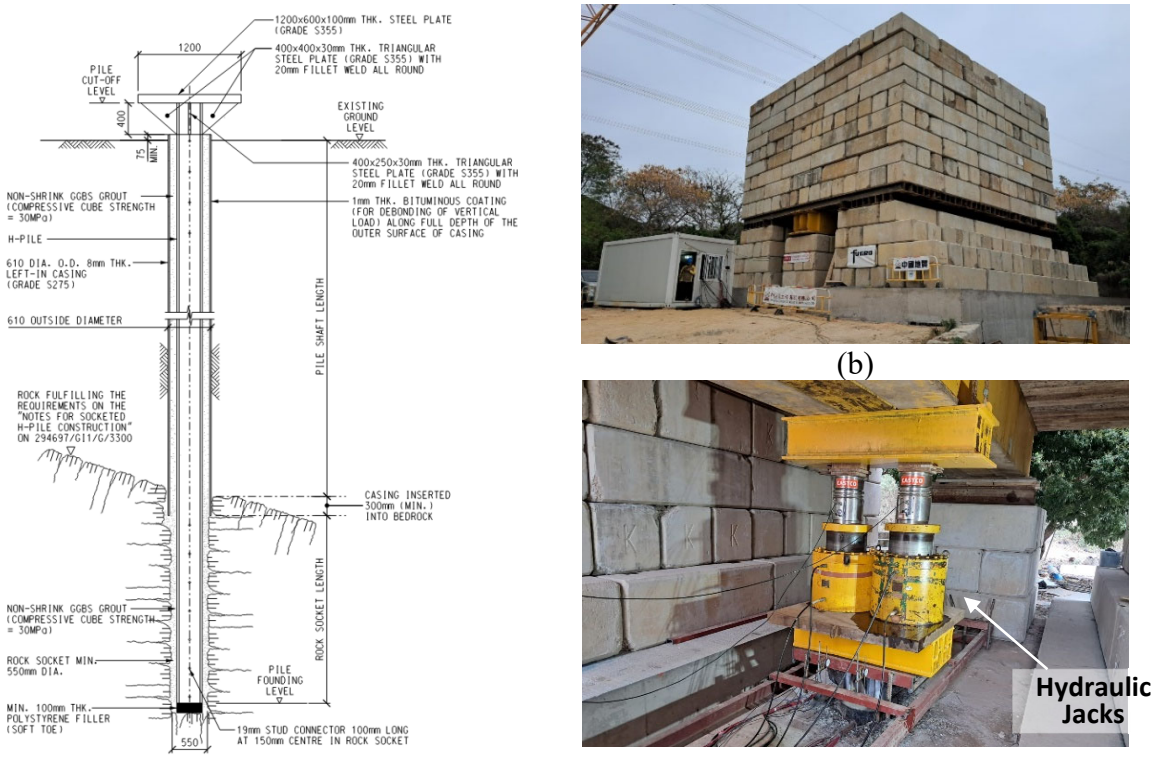
Table 3.3: Loading configuration for SHP-FK-P1 and SHP-FK-P2

	SHP-FK-P1	**SHP-FK-P2**
Method of load application	O-cell at Pile Base	Hydraulic Jacks at Pile Head
No. of Loading Cycles	4	2
Max. Load per Cycle (MN)	LC-1: 2.22; LC-2: 4.39; LC-3: 5.50; LC-4: 8.56	LC-1: 9.50; LC-2: 19.00
72 hr load-holding period	Yes	Yes
Load Cycle with Load-holding	LC-3	LC-2
Retained Load during Holding Period (MN)	5.50	19.00



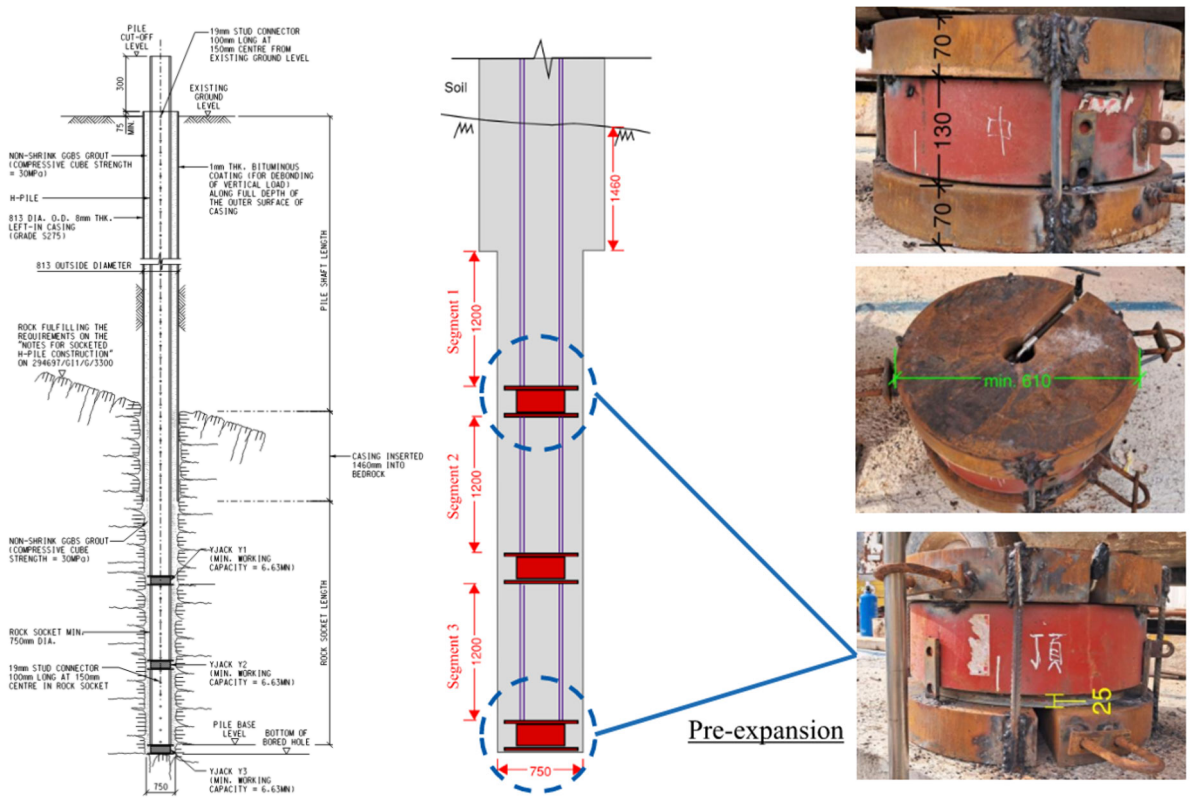
(a) (b) (c)

Figure 3.7: Details of trial pile SHP-FK-P1: (a) Schematic arrangement and key parameters; (b) Osterberg cell (O-cell); (c) Installation and configuration of O-cell



(a) (b) (c)

Figure 3.8: Details of trial pile SHP-FK-P2: (a) Schematic arrangement and key parameters; (b) Kentledge; (c) Hydraulic jacks for imposing load



(a) (b)

Figure 3.9: Details of trial pile SHP-FK-P3: (a) Schematic arrangement and key parameters; (b) Arrangement of the three Y-Jacks within rock socket

***SHP-FK-P3*:** The arrangement of trial pile SHP-FK-P3 is shown in Figure 3.9. This pile adopted a multi-level Y-Jack bi-directional testing system, with three flat jacks installed at different levels within an enlarged rock socket. The arrangement divided the socket into discrete test segments, allowing the resistance of individual socket zones and the pile-base response to be mobilised and interpreted separately within a single pile. This provided a more detailed assessment of load transfer than either a conventional head-down test or a single-level bi-directional test, and was a key innovative feature of the Fung Kong programme. The enlarged socket was provided to accommodate the jacks and associated instrumentation, while the lowest jack was pre-expanded before grouting to minimise base resistance when individual socket segments were being isolated. During testing, selected jacks were either pressurised, locked or released in a staged sequence to mobilise different resistance components.

The staged Y-Jack loading sequence is illustrated in Figure 3.10 and summarised in Table 3.4. In the table, “Press” denotes the jack being pressurised to apply bi-directional load, “Lock” denotes the jack acting as a load-transmitting part of the pile, and “Free” denotes the jack being released or pre-expanded so that load is not transmitted across that level. This staged arrangement allowed different socket segments and the pile-base response to be isolated within a single trial pile, while the detailed loading values and jack configurations are retained in Table 3.4 for reference.

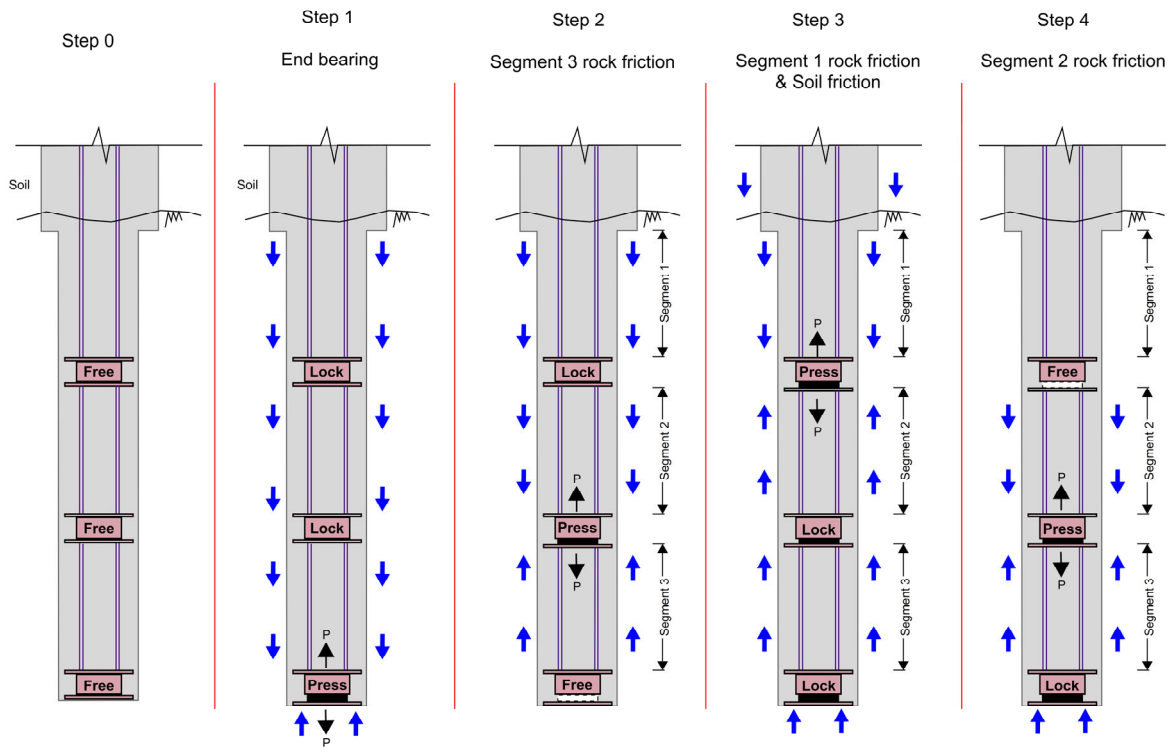


Figure 3.10: Y-Jack loading steps for SHP-FK-P3

Table 3.4: Design Sequence of Load Test for SHP-FK-P3

Step	Status of Y-Jack		
	Y1	Y2	Y3
0	Free	Free	Free
1	Lock	Lock	Press (6630 kN)
2	Lock	Press (6630 kN)	Free
3	Press (6630 kN)	Lock	Lock
4	Free	Press (6630 kN)	Lock

3.3.2 Value of multiple testing methods

A key value of the programme was its flexible use of different pile testing methods, rather than reliance on a single standard approach. The O-cell, conventional kentledge and multi-level Y-Jack tests each offered different practical advantages depending on the pile type, site constraints and resistance component to be examined. This allowed the programme to obtain field evidence from a wider range of test configurations and strengthened the overall basis for understanding pile behaviour in MS rock.

The approach also demonstrates an important shift towards more targeted and evidence-based testing. A conventional kentledge test can provide a familiar benchmark within local practice, an O-cell test can mobilise shaft and base resistance efficiently within the pile, and a multi-level Y-Jack test can isolate individual socket segments and pile-base response within a single test pile. With the flexibility of applying loading at selected level(s), this pile testing approach facilitates investigation of pile capacity of individual segments of piles for design optimization.

3.4 Fibre optic sensing technology

The use of optical fibre for sensing purposes has become increasingly popular in structural health monitoring, as physical quantities such as temperature, strain and vibration can be measured along the length of an optical fibre for long distances. Under certain conditions, the spatial resolutions of such measurements can reach centimetre or even millimetre levels. While conventional sensor systems usually involve point measurement sensors (e.g., thermal couples, strain gauges or accelerometers), a single fibre optic cable can provide continuous data along its length and hence serve the function of many individual point sensors. The use of fibre optic sensors also comes with other advantages, including their immunity to electromagnetic interference and resistance to corrosion, which make them suitable for long-term monitoring applications in civil infrastructure.

Light is transmitted along an optical fibre by total internal reflection. Scattering effects occur when light passes through a medium with non-uniform properties. Due to impurities in the fibre core, when a light signal is launched from one end of the fibre, backscattered lights are generated at each point of the fibre. Since the characteristics of backscattered lights are influenced by changes in the strains and temperatures experienced by the optical fibre, and the locations of the changes can be pinpointed through the speed of light and refractive index of the optical fibre, these characteristics open up opportunities for distributed sensing along the optical fibre cable.

A number of technologies in fibre optic sensing has been developed for sensing purposes over the past few decades, and each of them is associated with different features regarding spatial resolution, sensing distance, accuracy, etc. that make them suitable for various applications. For example, fibre Bragg grating (FBG) involves inscribing individual ‘gratings’ along the fibre, and the strain or temperature changes can be measured only at the locations of gratings. Hence, the corresponding measurements are not fully distributed. Brillouin optical time domain reflectometry (BOTDR) facilitates long sensing distances up to tens of kilometres, while the spatial resolution is usually in the order of 1 m. On the other hand, Brillouin optical time domain analysis (BOTDA) can achieve spatial resolution in centimetre levels, but requires both ends of the sensing cable to be connected to the equipment, which sometimes poses difficulties for construction site deployment, as no data can be retrieved with BOTDA if there is a breakage point along the cable.

For pile monitoring, the optical frequency domain reflectometry (OFDR) offers a viable option as it can achieve spatial resolutions of up to millimetres for strain and temperature measurements. Even if the cable is damaged, the data can be retrieved up to the point of breakage. Although the maximum sensing distance of most commercial OFDR equipment is around 100 – 150 m, this is usually adequate for foundation pile monitoring. The high spatial resolution also makes this technique particularly suitable for the S690 steel H-pile tests, as the main focus of the load test was on the behaviour of the rock sockets, which ranged from 2 – 6 m in length. Without the high spatial resolution, details of the strain developments in rock sockets could not be captured.

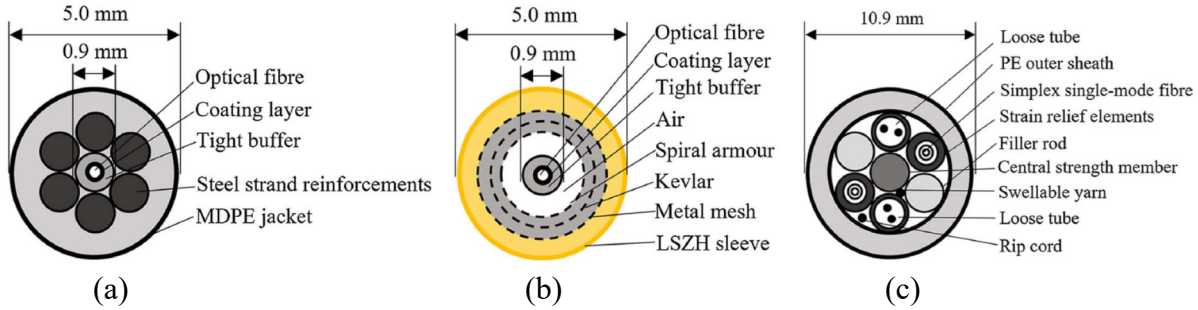


Figure 3.11: Examples of fibre optic sensors for distributed strain and temperature sensing

Although optical fibre cables are commonly used in telecommunication systems, the specific conditions of construction sites make it necessary to develop cables that are suitable for infrastructure monitoring. Figure 3.11 shows the cross sections of several types of optical fibre cables that had been successfully deployed in previous projects in Hong Kong. Figure 3.11(a) shows a tight-buffered single-mode cable that is usually adopted for strain sensing. The fragile fibre core protected by a steel strand–reinforced, medium density polyethylene (MDPE) jacket. The cable diameter is 5.0 mm, and the tight buffer ensures efficient strain transfer and the steel strand reinforcement prevents the sensing fibre from being damaged by site activities. Figure 3.11(b) shows a loose tube cable with a diameter of 5.0 mm, which is commonly used to monitor temperature changes. The fibre core is surrounded by four layers of filling materials including a spiral armour, Kevlar, metal mesh, and a low smoke zero-halogen (LSZH) sleeve that improve its robustness, and the space between the optical fibre and the spiral armour makes it mechanically strain-free. It is sometimes useful to bundle the two types together, as shown in Figure 3.11(c), so that both tight-buffed and loose-tube components can be contained in the same cable. In this case, the cable diameter is around 10.9 mm.

3.4.1 Benefits of fibre optic sensing in S690 trial piles

Unlike conventional strain gauges which also provide strain measurements at discrete locations of individual gauges, distributed sensing technologies facilitate measurements of continuous strain profiles along a single cable. This feature is particularly useful for pile instrumentation, as the strain variation at different depths can be clearly revealed and utilized to estimate the corresponding pile forces. Meanwhile, pile shaft resistance in various soil and rock strata can be derived based on the strain variations along the pile depth.

For S690 socketed H-pile tests, the focus was mainly on the pile behaviour within the rock-socketed sections, which ranged from 2 to 6 m in length. Through distributed fibre optic sensing, the continuity in strain profiles allowed the details of pile-rock interaction to be unveiled in high definition with a small number of sensing cables. In addition, fibre optic cables could be embedded into the grout surrounding the steel H-sections in the pile, thereby providing information on the interaction among the various materials of the piles.

At the Fung Kong test site, the piles were socketed into highly fractured meta-sedimentary rocks. These rock types could retain high variability in their properties at depths, due to the complex depositional and tectonic history. There had been limited studies in the past on the behaviour and capacities of piles in these rocks in the region. The large volumes of strain data by distributed sensing became useful to enhance the understanding on the variability of the materials and how this could affect foundation performance.

3.4.2 Details of fibre optic instrumentation at Fung Kong site

Fibre optic sensing cables were first attached to the S690 steel sections under the controlled environment of the steel factory. As mentioned earlier, there are multiple types of fibre optic sensing cables available in the market, and they involve the fibre core being surrounded by different materials depending on the intended purposes of instrumentation and the level of protection required. In this case, to increase the contact areas between the sensing cables and steel surface, the tests adopted a 0.9-mm strain sensing cable covered by two layers of glass-fibre woven fabric. The cables were attached to the inner surfaces of the flanges using slow-curing epoxy resin which saturated through the woven fabrics for effective bonding and strain transfer. To further protect the cables from potential damage during subsequent construction activities, a layer of foam tape was applied over the optic fibre cables, over which another protective layer of aluminium butyl tape was placed. Steel angle sections were spot-welded at the corners between the web and flanges to shield the optic fibre cables from excessive heat during welding and mechanical damage that might result from steel-grout interface displacements (Figure 3.12).

Besides, metal-reinforced strain sensing cables were also embedded in the grout body to monitor the strain developments in grout, to enhance the understanding on steel-grout-rock interaction effects. The steel-wire reinforcement provides protection to the inner fibre optic sensing cables against impacts during the grouting process, while the rough surface of the covering sleeve ensures strong bonding between the sensing cables and the grout. This type of sensing cable was also deployed successfully in several previous projects in Hong Kong, which monitoring of bored piles, diaphragm wall panels, deep cement mixing columns, etc. The typical cross section of the instrumented socketed S690 steel pile is shown in Figure 3.13.



Figure 3.12: Fibre optic sensors for strain monitoring in steel piles at Fung Kong

The steel piles involved multiple sections that needed to be spliced together by site welding. Technically, the fibre optic cables could be installed on various steel sections and then spliced together on site, but the connection points of sensing cables would require special protective measures. Therefore, in the Fung Kong pile tests, each steel section was instrumented with separate fibre optic cables that were individually connected to the equipment on the ground surface. This ensured efficient site operation procedures that caused minimal disruption to the pile installation.

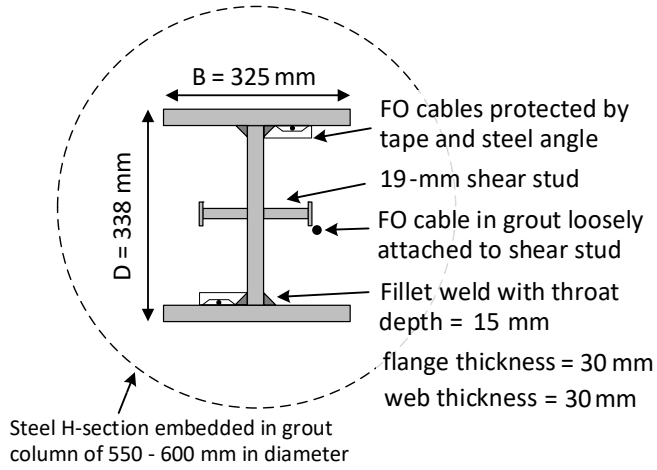


Figure 3.13: Cross section of instrumented socketed S690 steel pile with fibre optic sensors

3.4.3 Example results

Figure 3.14 shows examples of the fibre optic strain sensing results for two S690 steel test piles, i.e., SHP-FK-P1 and SHP-FK-P2, while Figure 3.15 shows the load-settlement response of SHP-FK-P2, demonstrating that both the settlement at maximum applied load and residual settlement upon unloading have fulfilled the corresponding acceptance criteria stipulated in the code of practice. The fibre optic sensing technique enabled fully continuous strain profiles to be revealed along the piles throughout the loading and unloading processes. Note that for SHP-FK-P1, the axial strains were only developed near the pile tip where the O-cell was located, and hence the strain profiles were shown only for the bottom steel H-section.

The strain profiles revealed information of soil-pile or rock-pile interactions along the pile depth, which were direct indicators of shaft friction features along the entire pile length. Within the soil layers, the left-in-place steel casing and the bitumen layer minimized the developments of soil-pile friction, resulting in axial strains that remained relatively unchanged. On the contrary, along the pile section socketed in rock, the grout was in direct contact with the rock and therefore high rock-pile shaft friction was mobilized, as illustrated by the steep change in axial strain profiles. Based on these results, the average shaft friction mobilized along the rock socket exceeded 1500 kPa, while the maximum friction value reached 3000 kPa without any signs of pile failure.

Specifically, for SHP-FK-P2 loaded by the kentledge system, the maximum test load reached 19,000 kN, which was 200% of the pile design capacity and reaching the yield strength of the steel sections. The measured maximum and residual settlements all fulfilled the corresponding requirements stipulated in the local code of practice. The performance of these piles demonstrated the feasibility of adopting high-strength steel piles as a viable foundation option. The benefits are discussed in detail through example calculations in multiple scenarios in the next section.

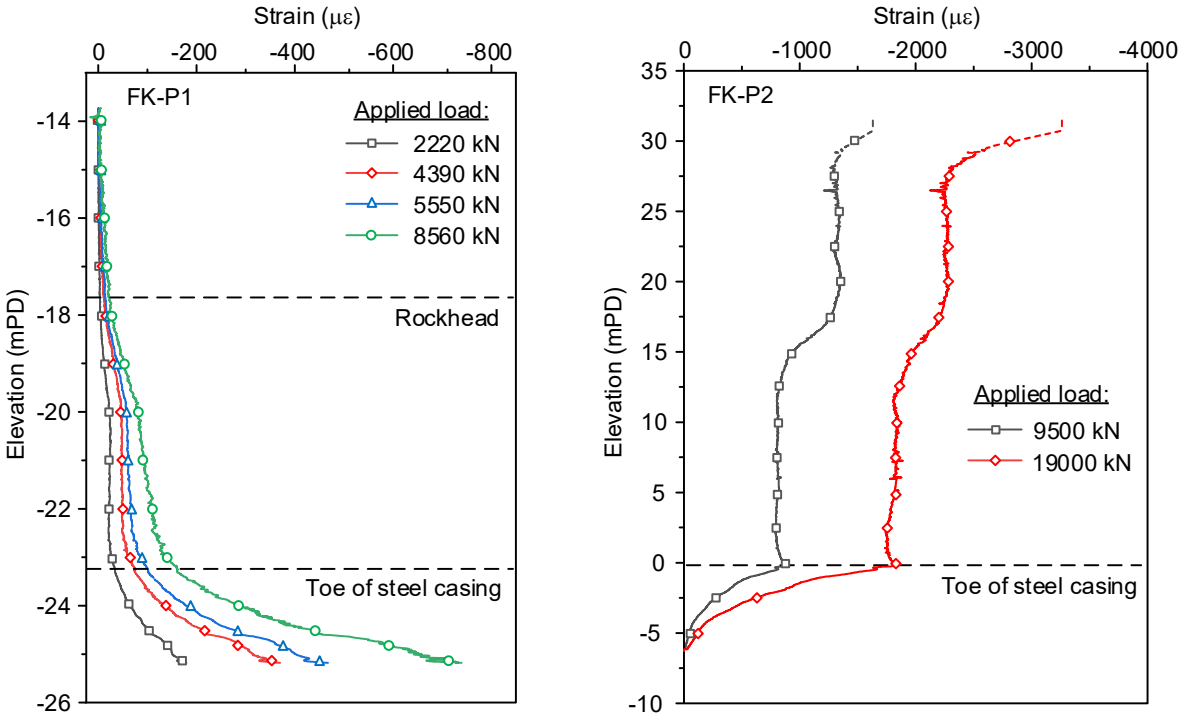


Figure 3.14: Examples of continuous strain profiles of the two loaded piles: (left) SHP-FK-P1 and (right) SHP-FK-P2

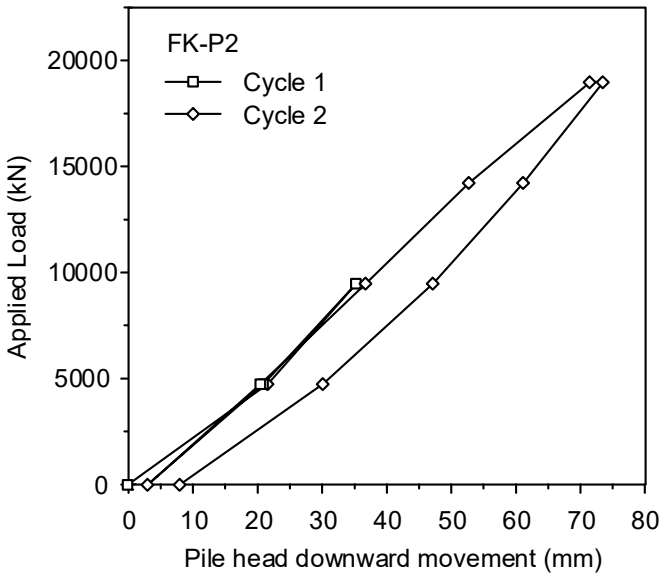


Figure 3.15: Load-settlement response of SHP-FK-P2 under two load cycles.

4. Unlocking potentials and benefits of high-strength steel H-piles – Design examples

The foundation system comprising pre-bored socketed H-piles is familiar to designers, contractors and approving authorities, and has become a well-established solution for dense urban development, reclamation areas and infrastructure works. This familiarity, together with enhanced properties of high-strength and ultra-high strength steel, provides a strong platform for innovation with an opportunity to improve the efficiency of a system already embedded in local practice. Meanwhile, the increasing scale and complexity of developments in Hong Kong place growing pressure on conventional pile layouts. Larger column loads, constrained works areas, congested substructures and deeper founding levels can lead to more piles, larger pile caps, increased drilling works and longer construction programmes. These issues are not only matters of structural capacity; they affect buildability, programme, site logistics, material use and the overall efficiency of foundation construction. Higher-strength steel piles offer a practical route to address these challenges.

While S450 is the conventional grade for socketed H-piles in Hong Kong, higher steel grades such as S690 and S960 increase the usable resistance of each H-pile and reduce the number of piles required to support the load. The resulting benefits may include smaller pile caps, fewer boreholes, reduced pile-head congestion and construction effort.

This section elucidates these potential benefits through design calculation and cost estimates of various typical foundation scenarios in Hong Kong. The potential use of S690 and S960 steel in socketed H-piles is considered relative to the conventional S450 baseline adopted in Hong Kong foundation design. Both full-length higher-grade piles and targeted hybrid arrangements are examined, with higher-grade steel used only where it provides the greatest benefit. The focus is on the practical opportunity, likely construction benefits and key limitations that require verification before the approach can be adopted in design.

4.1 Basis for a like-for-like comparison

A consistent reference foundation arrangement is used to compare the effect of steel grade on socketed H-pile performance. The pile section, socket diameter and ground profile are kept unchanged for the S450, S690 and S960 options. This allows the comparison to focus on the value that may be gained from the steel grade itself, rather than from changes in pile geometry or ground assumptions. The comparison recognises that a socketed H-pile is governed by both the steel section and the rock socket. Higher-strength steel can increase the structural resistance of the H-section, but it does not directly increase the bond capacity available from the surrounding rock. The practical benefit of adopting S690 or S960 therefore depends on whether the governing limit is structural or geotechnical, and whether sufficient socket length can be provided to fully capitalise on the enhanced steel strength.

The options are compared using practical foundation outcomes: the number of piles required, the load carried by each pile and the socket length required. This keeps the assessment focused on the potential construction benefits, including reduced drilling, reduced pile-head congestion and a smaller pile-cap footprint. More detailed assumptions on pile geometry, pile behaviour and rock socket capacity are set out in the following subsections.

A single reference pile section is used for all three grades so that the effect of steel grade is isolated. The section is a 305 × 305 × 223 kg/m H-section (Figure 4.1), with the key properties summarised in Table 4.1. The section geometry and modulus of elasticity are kept constant for S450, S690 and S960 sections.

Table 4.1: Section properties and geometry of the reference pile

Parameter	Symbol	Value	Unit
Gross cross-sectional area	A	28,500	mm²
Second moment of area, major axis	I_x	52,800	cm⁴
Second moment of area, minor axis	I_y	17,600	cm⁴
Radius of gyration, minor axis	r_y	7.87	cm
Elastic section modulus, major axis	S_x	3,650	cm³
Elastic section modulus, minor axis	S_y	1,680	cm³
Modulus of elasticity	E	205	GPa
Distance between Ground Surface and Rock Head	L	44	m
Socket diameter	D_s	550	mm

Above the rock socket, the H-section is laterally supported by the surrounding ground and acts as a slender compression member. As a result, the usable structural resistance is influenced by both steel grade and buckling behaviour. Increasing the steel grade improves the resistance of the H-section, but the gain is moderated because the pile geometry, stiffness and restraint conditions remain unchanged.

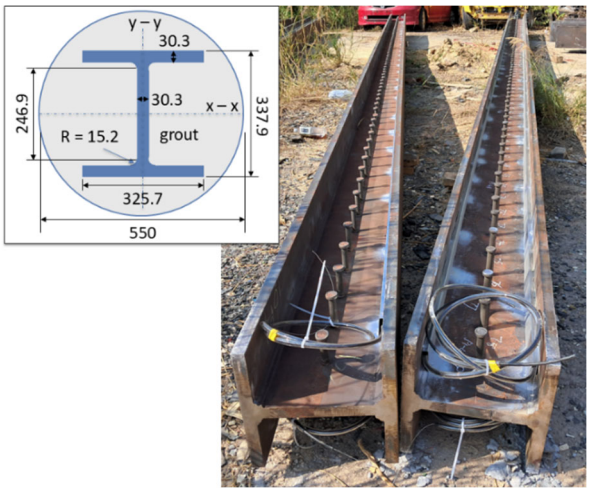


Figure 4.1: Cross-section and photograph of H-Pile prior to installation (dimensions in mm)

For the reference pile arrangement, the upper portion of the pile within $4T$, where T is the characteristic length of the soil-pile system, is treated as the zone most affected by bending. Below this zone, the pile response is principally governed by axial compression. This distinction is important because it provides the basis for a 'hybrid' pile arrangement, where higher-grade steel is used only in the upper bending-critical zone rather than along the full pile length[1]. The adopted strength parameters for S450, S690 and S960 are summarised in Table 4.2.

Note 1: This hybrid concept originated from a schematic footbridge design for a project of East Development Office of CEDD

Table 4.2: Structural strength parameters for reference pile section

Grade	Nominal grade designation: MPa	Design strength p_y: MPa	Buckling-reduced member compressive strength p_c: MPa
S450	450	430	354
S690	690	690	506
S960	960	960	646

The pile-capacity comparison considers the structural adequacy of the steel H-section and the geotechnical resistance developed through the grouted rock socket as separate requirements. The structural assessment comprises two checks. First, under working load, the average axial compressive stress in the steel section is limited to 50% of the adopted design strength p_y, in accordance with the Code of Practice for Foundations (BD, 2024).

$$\frac{N_{\mathrm{W}}}{A_{\mathrm{s}}} \leq 0.5 p_y$$

where

N_{W} = axial force under working load
A_{s} = cross-sectional area of the steel H-section

Second, the member resistance of the H-section is checked in accordance with the Steel Code (BD, 2023). Where axial load is combined with lateral load, an interaction check is used so that combined effect on structural capacity is considered. This provides a consistent way to compare the S450, S690 and S960 options under the different loading conditions considered:

$$\frac{N_{\mathrm{L}}(DL{+}LL + NSF)}{P_{\mathrm{c}}} + \frac{N_{\mathrm{M}} M_{\mathrm{x}}}{M_{\mathrm{cx}}} + \frac{N_{\mathrm{M}} M_{\mathrm{y}}}{M_{\mathrm{cy}}} \leq 1$$

where

N_{L} = load partial factor, taken as 1.4/1.6 for dead/live nature of the load
N_{M} = moment partial factor, taken as 1.4/1.6 for dead/live nature of the moment
NSF = negative skin friction
M_{x} = design moment about the major axis
M_{y} = design moment about the minor axis
M_{cx} = moment capacity about the major axis
M_{cy} = moment capacity about the minor axis
P_{c} = buckling-reduced compression resistance of the steel H-section
DL = dead load
LL = live load

The interaction check defines the service load that can be carried by each pile after allowing for the relevant load and moment factors. The moment capacities about the major and minor axes are derived from the section modulus and design strength. Negative skin friction is treated as an additional axial demand on the pile.

The geotechnical capacity is developed through bonding along the grouted rock socket. An allowable bond stress of 700 kPa recommended by the GEO TGN No. 53 (Issue 2) (GEO, 2026) is adopted for the metasedimentary rock Category 2b, with end bearing at the socket base neglected. The required socket length for a given pile demand is therefore estimated as follows:

$$L_{\text{socket}} = \frac{P}{\tau_{\text{allow}}\,\pi\,D_{\text{s}}}$$

where

L_{socket} = rock socket length
P = axial load exerted on the pile
τ_{allow} = bond at the interface between the rock and the socket
D_{s} = diameter of the grouted rock socket

GEO studies indicate that the enhanced rock socket parameters may be used where supported by suitable ground investigation, rock quality assessment and site-specific verification, as indicated by the GEO TGN No. 53 (Issue 2) (GEO, 2026). Adoption of such enhanced parameters could increase the geotechnical resistance and thereby avoid a disproportionate increase in rock socket length when utilising the higher structural capacities of S690 and S960 steel.

In addition, for comparison purposes, qualifying rock is assumed to extend to sufficient depth below rockhead, so that the socket length can be increased as required. The governing pile capacity is therefore controlled by the lesser of the structural capacity and the geotechnical capacity that can be developed. This distinction is central to the assessment: higher-strength steel may reduce pile numbers, but the benefit can only be realised where sufficient socket length and suitable rock are available.

4.2 Application scenarios and practical benefits for steel grades S690 and S960

Four scenarios are considered to examine the performance of higher-strength steel piles under different loading conditions. All piles share the common basis established above, with foundations comprising S450 socketed H-piles adopted as the reference case. For each scenario, the required number of piles, construction duration, cost, and carbon footprint were evaluated for foundations comprising S690 and S960 socketed H-piles for comparison to the reference.

The construction duration was assumed to be proportional to the number of piles required, as the construction methodology and installation procedures were considered identical across all scenarios. The carbon footprint was evaluated based on the embodied carbon associated with material production, including pile cap concrete, rock-socket grout, and structural steel. Embodied carbon emissions were estimated using emission factors of 2.1 $kgCO_2e/kg$ for structural steel and 0.166 $kgCO_2e/kg$ for concrete, adopted from the *Inventory of Carbon and Energy (ICE) Database* developed by Hammond and Jones (2011).

4.2.1 Scenario 1: Pile foundation using S450, S690 and S960 piles for a building

Scenario 1 involves a pile foundation design for a 29-storey building, with a 2-storey podium and a 2-level basement (Figure 4.2a). Rockhead is assumed to be 44 m below ground level. The superstructure is assumed to be supported by 30 columns on a 6 × 5 grid at 7 m centres (Figure 4.2b), and each column is founded on a pile group. The reference case uses S450 steel H-piles with an assumed floor load of 25 kPa. The column selected for analysis transfers a design load of about 35,000 kN to the foundation. Following the abovementioned procedures, this column requires six S450 H-piles, each with a 5-m rock socket, resulting in a total pile length of 49 m. The entire foundation contains 140 number of S450 socketed H-piles.

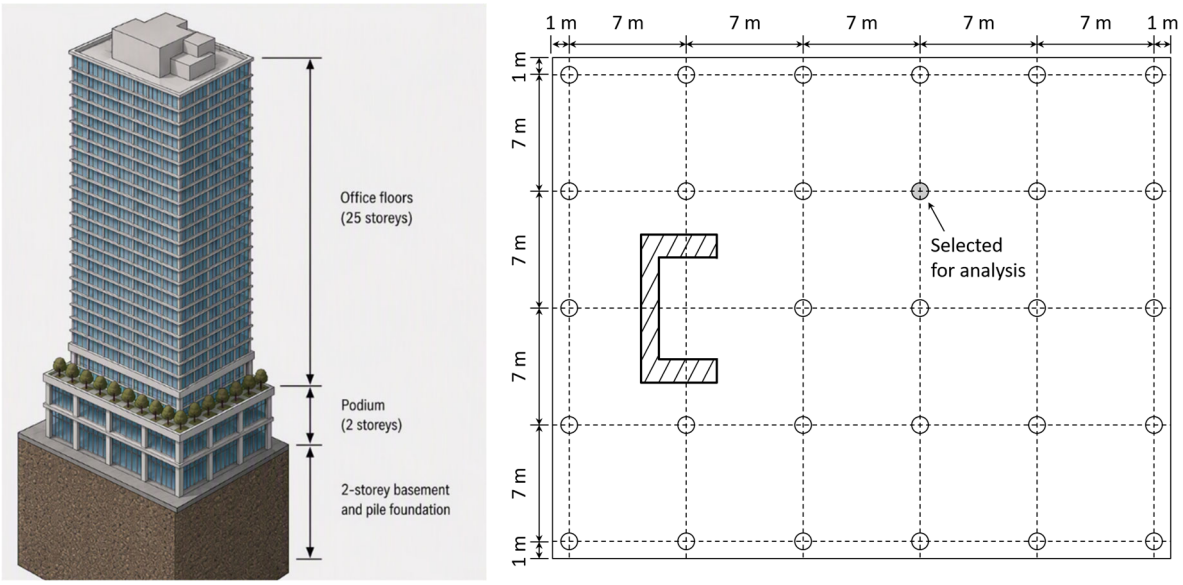


Figure 4.2: Schematic illustration of (a) Isometric view of building and (b) Column layout

The same assessment was carried out for S690 and S960 socketed H-piles. For the column selected for analysis, four S690 piles and three S960 piles were required to satisfy the design demand. Accordingly, the overall foundation system comprised 98 S690 H-piles and 72 S960 H-piles, respectively. The typical pile arrangements adopted for the representative column using S450, S690 and S960 H-piles are schematically shown in Figure 4.3.

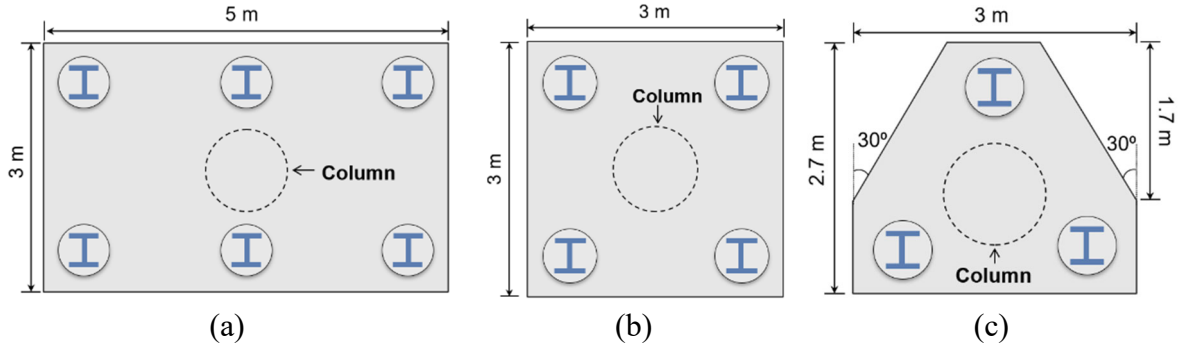


Figure 4.3: Comparison of pile arrangements using (a) S450, (b) S690 and (c) S960 H-Piles

Figure 4.4 compares the number of piles, pile lengths, construction time, cost and carbon emissions of each option. The required pile lengths for the S450, S690 and S960 H-piles are 49.1 m, 52.1 m and 55.3 m, respectively. S690 and S960 steel piles reduce the construction time of the whole pile foundation to 70% and 51% of the reference case. The cost falls to 82% and 75%, and carbon emissions fall to 74% and 58%. Cost and carbon emissions fall by less than the number of piles because high-strength steel has a higher unit cost and higher embodied carbon. High-strength steel H-piles, particularly S960, can significantly reduce the number of piles, the construction programme and carbon emissions, leading to additional cost saving.

The socket lengths adopted in the above comparison are governed by the allowable rock–grout bond stress. The *Code of Practice for Foundations 2017* (BD, 2024) adopted a single presumed allowable bond stress of 300 kPa under compression for all Category 2 meta-sedimentary rock, without differentiating rock quality. The recently promulgated, GEO TGN No. 53 (Issue 2) (GEO, 2026) introduces a more refined classification, with presumed allowable bond stresses

of 1,000 kPa, 700 kPa and 300 kPa for Categories 2a, 2b and 2c, respectively, and 1,000 kPa for Categories 1a and 1b. The revised provisions therefore retain the previous value for poorer Category 2c rock while permitting higher bond stresses, and consequently shorter required bond lengths, where better-quality rock is demonstrated.

For the same pile demand and socket diameter, the required bond length is inversely proportional to the allowable bond stress. Accordingly, adopting 700 kPa rather than 300 kPa reduces the required bond length by approximately 57%, while a value of 1,000 kPa gives a reduction of 70%. Across the S450, S690 and S960 options considered in Scenario 1, the required bond lengths range from approximately 5 m to 11 m per pile at 700 kPa, compared with approximately 12 m to 26 m per pile at 300 kPa. GEO TGN No. 53 (Issue 2) (GEO, 2026) therefore enables the enhanced structural capacities of S690 and S960 piles to be utilised with shorter and more practicable bond lengths, provided that the applicable rock category is substantiated through suitable ground investigation, rock mass characterisation and site-specific verification.

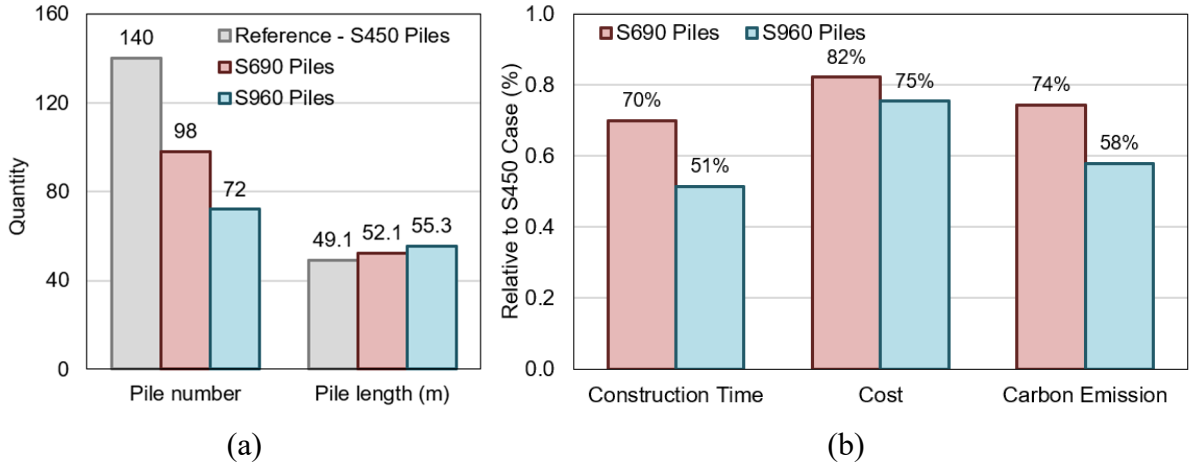


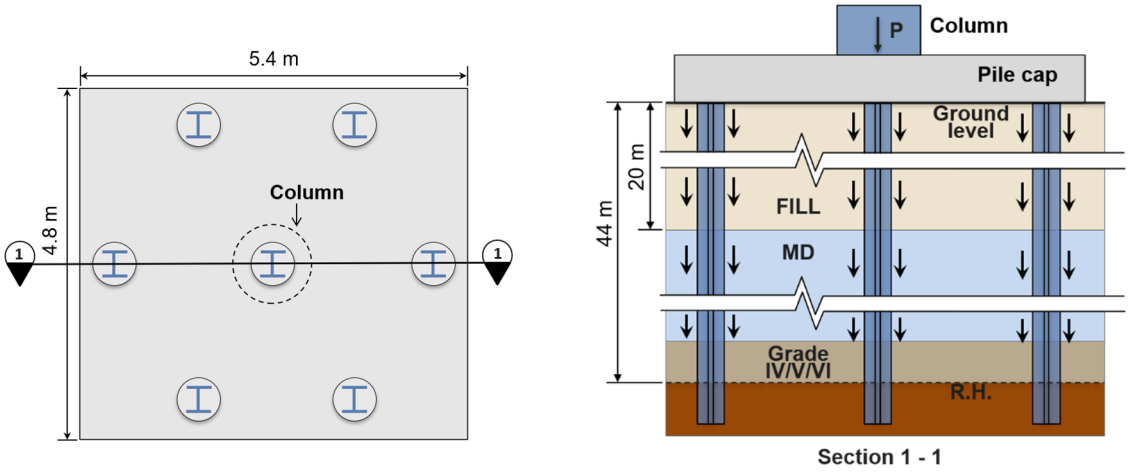
Figure 4.4: Performance of S450, S690 and S960 H-pile foundations for Scenario 1: Comparison of (a) Pile numbers and Length; (b) Normalised construction time, cost and carbon footprint

4.2.2 Scenario 2: Socketed H-piles under vertical load with negative skin friction

Scenario 2 is a hypothetical pile design beneath a single column at a typical reclamation site, such as the one shown in Figure 4.5, where fill overlies compressible marine deposits as schematically shown in Figure 4.6. As the marine deposits consolidate, the surrounding ground settles relative to the piles and mobilises negative skin friction (NSF) along the pile shafts. A column service load of 35,000 kN is adopted, with an assumed NSF of 1,500 kN acting on each pile.



Figure 4.5: Reclamation Site at Tung Chung New Town Extension (Source: CEDD)

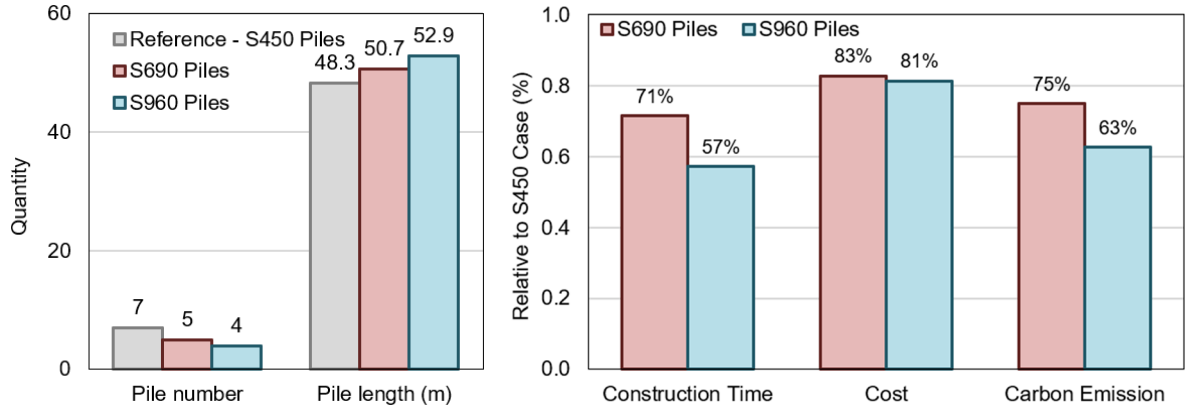


(a) (b)

Figure 4.6: Schematic illustration of reference pile configuration subjected to NSF induced by soft layer consolidation: (a) Layouts of columns and piles; (b) Sectional view

According to the calculation results, the S450 reference case requires seven piles. This reduces to five piles with S690 and four piles with S960. Because NSF acts on each pile individually, a smaller pile group attracts a smaller total downdrag force, which falls from 10,500 kN to 7,500 kN and 6,000 kN respectively. The benefit is therefore compounded as higher-grade steel leads to reduction in the number of piles required, and the smaller pile group in turn reduces the total downdrag load.

Figure 4.7 compares the pile number, pile length construction time, cost and carbon emissions of each option. The required pile lengths for the S450, S690 and S960 H-piles are 48.3 m, 50.7 m and 52.9 m, respectively. S690 and S960 piles reduce the construction time to 71% and 57% of the reference case. Cost falls to 83% and 81%, and carbon emissions fall to 75% and 63%. S690 and S960 piles increase the usable resistance of each pile where the structural mechanism governs. This is particularly relevant to constrained urban sites, heavily loaded pile caps and reclamation areas, where fewer piles also reduce the total NSF attracted by the group.



(a) (b)

Figure 4.7: Performance of S450, S690 and S960 H-pile foundations for Scenario 2: Comparison of (a) Pile numbers and Length; (b) Normalised construction time, cost and carbon footprint

4.2.3 Scenario 3: Hybrid upper-zone H-piles under combined axial load and bending

Scenario 3 considers foundations where differing ground levels on either side, such as those associated with a semi-basement, generate unbalanced lateral earth pressures. As illustrated in Figure 4.8, this imbalance induces a moment at the foundation head, causing the socketed H-piles to resist combined axial load and bending. The additional bending demand reduces the axial structural capacity available from each pile and may therefore increase the number of piles required.

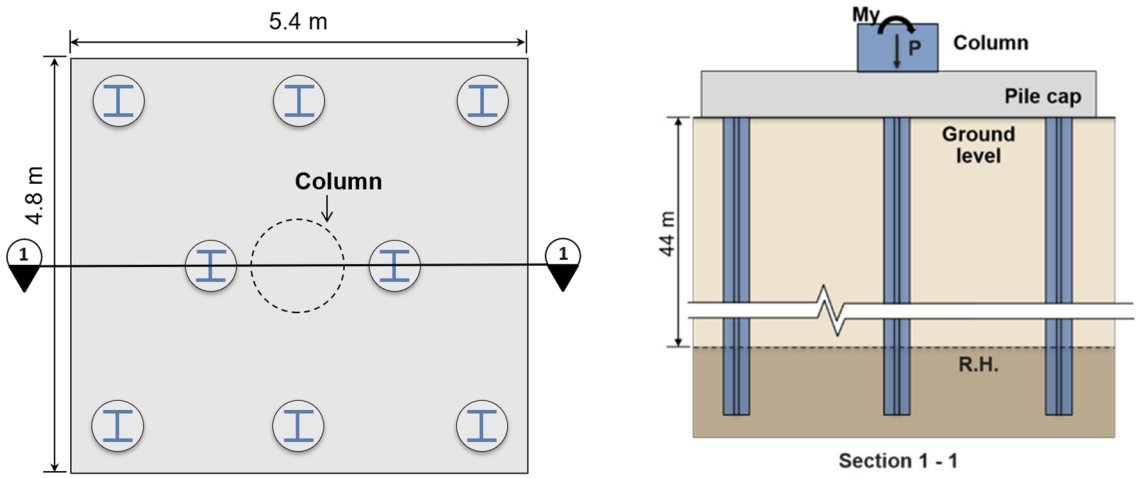
Since most of the bending response is concentrated within the upper $4T$ zone, a hybrid pile arrangement, inspired by a recent project of the East Development Office of CEDD, is considered. In this arrangement, S690 or S960 steel is used over the upper $4T$ zone of the pile, while S450 steel is retained along the lower shaft, which is subjected mainly to axial compression. T is the characteristic length of the soil-pile system and is defined as $T = (EI/n_h)^{1/5}$, where EI is the flexural rigidity of the pile and n_h is the coefficient of horizontal subgrade reaction increasing linearly with depth. The reference foundation configuration and the proposed hybrid pile arrangement are shown schematically in Figure 4.9.

To represent this practical condition, a vertical foundation load of 35,000 kN and a pile-head moment of 350 kNm arising from the unbalanced lateral load are adopted. Following the assessment procedure described earlier, the S450 reference case requires eight piles, as shown in Figure 4.9(a). By using higher-strength steel within the upper $4T$ zone, the required number reduces from eight piles for the reference S450 case to six piles for S690/S450 hybrid option, as shown in Figure 4.9(b).

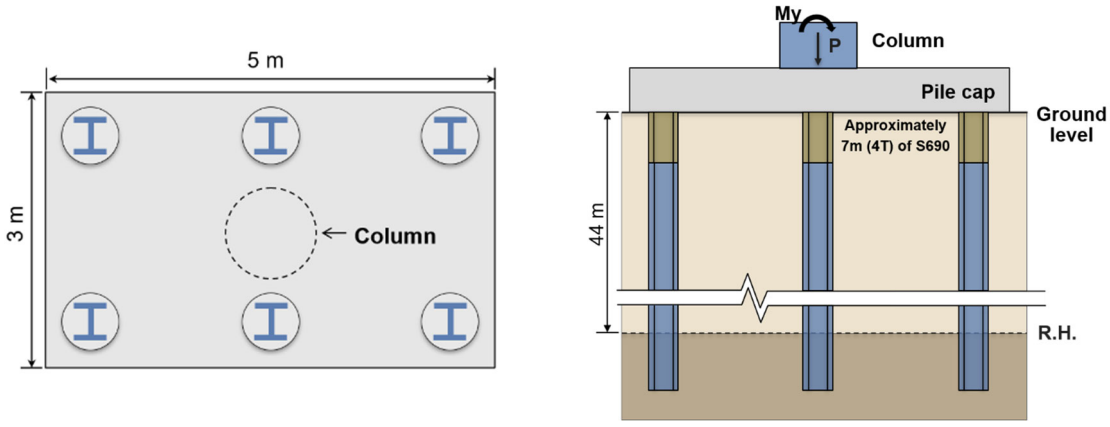
Hybrid pile option can effectively reduce the construction time and carbon emissions to approximately 75% of the S450 reference case. The corresponding costs are reduced to 78%. High-strength steel is used only in the upper segment, so these savings need much less premium steel than full-length S690 piles. This reduces procurement demand and fabrication cost. However, the splice between the two grades needs suitable welding procedures and quality control. The hybrid arrangement is therefore best suited where bending is concentrated near the pile head, with the lower shaft mainly axially loaded.



Figure 4.8: Illustration of a foundation subjected to moment from unbalanced earth pressure



(a)



(b)

Figure 4.9: Schematic Illustration of reference pile configuration and hybrid piles: (a) S450 reference case; (b) S690/S450 hybrid option

4.2.4 Scenario 4: High-strength steel H-piles as alternatives to large-diameter bored piles

Scenario 4 considers a heavily loaded column carrying an axial load of approximately 72,000 kN, around twice the load considered in Scenario 1 and is broadly representative of a major column in a high-rise building. At this level of loading, eleven S450 socketed H-piles would be required beneath a single pile cap, resulting in a large pile group, increased pile-cap dimensions, and greater demands on excavation and foundation construction. On constrained urban sites, the larger foundation footprint may also complicate coordination with adjacent basement and substructure elements.

Under these conditions, large-diameter bored piles are commonly adopted in Hong Kong practice because of their high individual pile capacities. However, bored piles require large-diameter excavation, temporary casing installation and substantial volumes of in-situ concrete. Construction may also become more challenging where corestones or other hard underground obstructions are encountered, as these can impede bore advancement and require additional drilling or obstruction-removal measures. While such obstructions may also affect pre-bored socketed H-piles, their smaller bore diameter generally allows localised treatment to be undertaken more readily. Consequently, adopting bored piles in place of socketed H-piles may introduce additional construction complexity and programme implications.

The use of higher-strength steel provides a potential means of extending the practical application range of socketed H-piles into this higher loading regime. For the assumed column load of approximately 72,000 kN, the required number of piles reduces from eleven using S450 steel to eight using S690 steel and six using S960 steel piles (Figure 4.10). The reduction in pile numbers leads directly to smaller pile caps, fewer pre-bored holes and rock sockets, reduced construction effort, and a more compact foundation arrangement. These results suggest that S690 and S960 steel can significantly enhance the competitiveness of socketed H-piles for heavily loaded foundations, reducing the need to adopt large-diameter bored piles solely to achieve the required axial capacity.

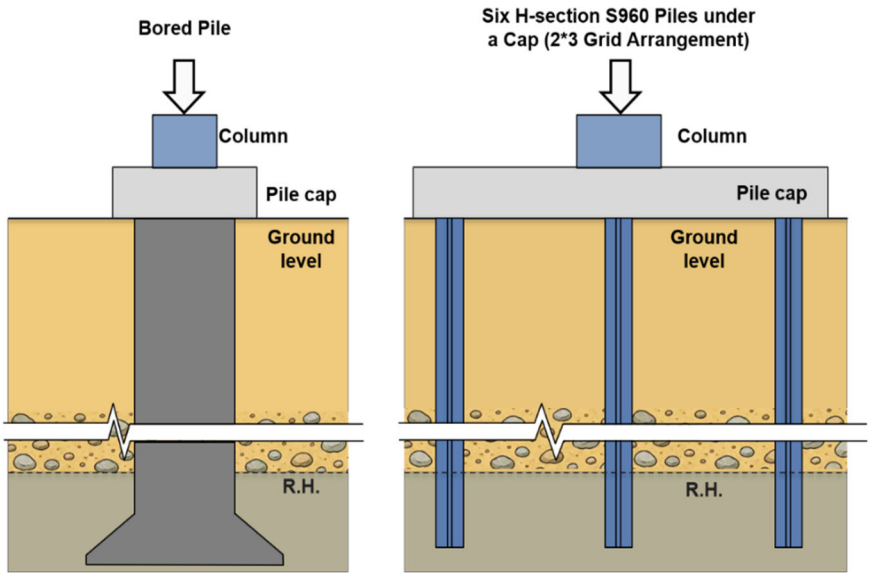


Figure 4.10: Schematics of the replacement of a conventional bored pile with S960 H-pile group

4.3 Potential benefits of high-strength steel piles

High-strength steel offers a practical way to deliver more efficient socketed H-pile foundations without departing from a system already well established in Hong Kong. Across the four scenarios, S690 and S960 reduce the number of piles, pre-bored holes and rock sockets required, creating smaller pile caps with less pile-head congestion. The assessments for Scenarios 1 to 3 also indicate shorter construction programmes and lower embodied carbon. In reclamation areas, reducing the number of piles provides the added benefit of lowering the total negative skin friction attracted by the pile group.

The hybrid pile concept demonstrates how higher-strength steel can be deployed selectively rather than throughout the full pile length. Using S690 or S960 within the upper 4T bending-critical zone, while retaining S450 along the predominantly axially loaded lower shaft, concentrates the premium material where it delivers the greatest structural benefit. This approach can reduce pile numbers while limiting the quantity of higher-strength steel required, providing a practical and optimised pathway for introducing advanced steel grades into routine foundation design.

Higher-strength steel could also expand the application of socketed H-piles to more heavily loaded foundations. For the approximately 72,000 kN column load considered in Scenario 4, the required pile group reduces from eleven S450 piles to eight S690 piles or six S960 piles. This creates a more compact foundation and offers a potential alternative where a large-diameter bored pile might otherwise be selected.

Together, these scenarios show that S690 and S960 can enhance the capacity, buildability and resource efficiency of socketed H-pile foundations. The next step towards wider adoption is to validate the proposed applications through project-specific design, detailing, constructability assessment and field trials, with particular attention to rock socket capacity, steel-grade transitions and installation control.

5. Summary and way forward

The three full-scale pile tests at Fung Kong demonstrated the viability of adopting high-strength steel as pre-bored socketed H-piles. The trials provided valuable practical experience in the construction of S690 steel piles, particularly in site welding, inspection and quality assurance, together with the placement of GGBS grout. Pile performance and rock socket behaviour were assessed using conventional kentledge, single O-cell and multi-level Y-Jack testing methods, supported by distributed fibre optic sensing to characterise strain distributions and load transfer. The construction procedures, inspection and pile test results satisfied the relevant requirements adopted for the trials, providing a practical reference for the application of high-strength steel in pile foundations.

The reported field tests have indicated that high bond stress can be mobilised between the MS rocks and grout surrounding the H-sections of the pile. Without any signs of pile failure, these mobilised bond stress values exceeded the presumed allowable values stipulated in the earlier foundation design provisions, which reflected the limited test data available at the time. The results of the wider trial piling programme provided the technical basis for the revised allowable bond stress values promulgated in GEO TGN No. 53 (Issue 2). This update, together with the construction and testing experience gained at Fung Kong, supports the application of high-strength steel piles, subject to the geological conditions and design requirements of individual projects.

Besides rock-grout friction, the bond stresses between steel H-section and the surrounding grout also govern the design of pre-bored socketed H-piles. Both laboratory and field tests have demonstrated that steel–grout bond stresses higher than the values prescribed in the design codes can be mobilised. PolyU is undertaking a separate comprehensive test programme to investigate the effects of shear connector/shear stud arrangements along the H-sections on bond development and overall pile performance. These investigations may provide further insights to support the effective utilisation of the higher structural capacity of high-strength steel piles.

The design examples illustrate the potential benefits of adopting S690 and S960 steel across different foundation scenarios, including fewer piles, smaller pile caps and reduced construction effort. The assessments also indicate opportunities to reduce construction time, costs and embodied carbon, subject to the assumptions and conditions of each scenario. Hybrid arrangements offer a further opportunity to use higher-strength steel selectively where it provides the greatest structural benefit. These examples complement the S690 field trials, while their application to individual projects requires consideration of the governing structural and geotechnical capacities, site constraints and construction requirements.

The way forward is to translate the experience gained from the trials into wider, project-specific application of high-strength steel pile foundations. Early consideration of this option during foundation planning and design would enable its potential benefits to be assessed against conventional alternatives. Drawing on the updated guidance, construction procedures, quality assurance measures and testing experience presented in this publication, practitioners can make informed decisions on its suitability for their projects and support its wider adoption, contributing to more productive, cost-effective and resource-efficient foundation construction in Hong Kong.

References

AASHTO (2007). *AASHTO LRFD Bridge Design Specifications.* American Association of State Highway and Transportation Officials, Washington, DC.

Bieniawski, Z.T. (1974). Geomechanics classification of rock masses and its application in tunnelling. *Proceedings of the Third International Congress of the International Society for Rock Mechanics*, Denver, Vol. 2A, pp. 27-32.

BD (2023). *Code of Practice for the Structural Use of Steel 2011 (2023 Edition)*. Buildings Department, Hong Kong.

BD (2024). *Code of Practice for Foundations 2017 (2024 Edition)*. Buildings Department, Hong Kong.

BSI (2020). *Code of practice for foundations*. BS 8004:2015+A1:2020. British Standards Institution, London.

CEDD and BTRi (2026). *Technical Guidelines for Robotic Welding Operations of Structural Steel in Construction.* Civil Engineering and Development Department and Building Technology Research Institute, Hong Kong.

CGS (2006). *Canadian Foundation Engineering Manual.* Canadian Geotechnical Society, Surrey.

Chiu, K.Y.K. and Sze, E.H.Y. (2004). Trial piles with high percentage GGBS. *Proceedings of The HKIE Geotechnical Division 44th Annual Seminar - Elevating Geotechnical Excellence: Novel Practices & Innovative Solutions*, 7 p.

Chung, K.F. (2022). Effective use of high-strength S690 to S960 steel in construction. *Hong Kong Engineer,* Vol. 50.

GEO (2006). *Foundation Design and Construction.* (GEO Publication No. 1/2006). Geotechnical Engineering Office, Hong Kong.

GEO (2011). *Final Report on Durability and Strength Development of Ground Granulated Blastfurnace Slag Concrete.* GEO Report No. 258, Geotechnical Engineering Office, Hong Kong.

GEO (2022). *San Tin : Solid and Superficial Geology (1:20 000 map) (2022, Edition II), 1 map*. Geotechnical Engineering Office, Hong Kong.

GEO (2026). *Supplementary Guidelines for Foundation Design and Construction* (Technical Guidance Note No. 53, Issue 2). Geotechnical Engineering Office, Hong Kong.

Hammond, G. and Jones, C. (2011). *Inventory of Carbon and Energy (ICE) Database*. Sustainable Energy Research Team, Department of Mechanical Engineering, University of Bath, UK.

Higgins, D. (2007). Briefing: GGBS and Sustainability. *Proceedings of the Institution of Civil Engineers – Construction Materials*, Vol. 160 (3), 99-101.

CEDD INNOVATION SERIES

